CHEMISTRY
A EUROPEAN JOURNAL

Low-Melting, Low-Viscous, Hydrophobic Ionic Liquids: Aliphatic Quaternary Ammonium Salts with Perfluoroalkyltrifluoroborates

Zhi-Bin Zhou, Hajime Matsumoto,* and Kuniaki Tatsumi[a]

Abstract: A novel class of low-melting, hydrophobic ionic liquids based on relatively small aliphatic quaternary ammonium cations ($[R^1R^2R^3NR]^+$, wherein R^1, R^2, R^3 = CH_3 or C_2H_5, R = *n*-C_3H_7, *n*-C_4H_9, $CH_2CH_2OCH_3$) and perfluoroalkyltrifluoroborate anions ($[R_FBF_3]^-$, R_F = CF_3, C_2F_5, *n*-C_3F_7, *n*-C_4F_9) have been prepared and characterized. The important physicochemical and electrochemical properties of these salts, including melting point, glass transition, viscosity, density, ionic conductivity, thermal and electrochemical stability, have been determined and comparatively studied with those based on the corresponding $[BF_4]^-$ and $[(CF_3SO_2)_2N]^-$ salts. The influence of the structure variation in the quaternary ammonium cation and perfluoroalkyltrifluoroborate ($[R_FBF_3]^-$) anion on the above physicochemical properties is discussed. Most of these salts are liquids at 25 °C and exhibit low viscosities (58–210 cP at 25 °C) and moderate conductivities (1.1–3.8 mS cm^{-1}). The electrochemical windows of these salts are much larger than those of the corresponding 1,3-dialkyimidazolium salts. Additionally, a number of $[R_FBF_3]^-$ salts exhibit plastic crystal behavior.

Keywords: electrochemistry · ionic liquids · perfluoroalkyltrifluoroborates · plastic crystals · quaternary ammonium

Introduction

In recent years, ionic liquids (ILs) have received a considerable upsurge of interest as new media for organic reactions,[1] biocatalytic transformations,[2] and separation technologies,[3] and as potential electrolytes for various electrochemical devices, such as Li-ion batteries,[4,5] dye-sensitized solar cells,[6] electrochemical actuators, electrochromic windows, and numerical displays.[7] This is mainly attributable to their superior properties over conventional volatile organic solvents and electrolytes, such as nonvolatility, nonflammability, high thermal stability, and wide liquid ranges.[1–3,5,8]

Currently, the basic understanding and applications of ILs are largely governed by imidazolium systems because the ILs based on the imidazolium cations, especially 1,3-dialkylimidazolium cations, have been empirically demonstrated to afford low viscosities and high conductivities, which are the key requirements for ILs as new reaction media or electrolytes to replace conventional materials.[1–8] However, these ILs cannot be used as electrolytes for high-energy electrochemical devices, such as 4 V class Li batteries (i.e. Li metal or carbon used as anode material) because of the electrochemical instability of the 1,3-dialkylimidazolium cations (i.e. the cathodic limit is $\approx$1 V versus Li^+/Li, which excludes the use of Li metal or carbon as anode).[4,9] Compared with the 1,3-dialkylimidazolium cations, saturated quaternary ammoniums are more resistant against oxidation and reduction, thereby their ILs with electrochemically stable anions, such as bis(trifluoromethanesulfonyl)imide $[(CF_3SO_2)_2N]^-$ ($TFSI^-$), have much larger electrochemical windows than the corresponding 1,3-dialkylimidazolium compounds.[9] Furthermore, recent studies have shown that the ILs based on the quarternary ammonium (QA) and robust anions, such as $TFSI^-$ and $[BF_4]^-$, have sufficient electrochemical stability to support them as possible safety electrolytes (nonvolatile and nonflammable) for high-energy devices, such as Li batteries[10–12] and double-layer capacitors,[13] and for electropositive metal deposition, such as Li and Eu.[9b,14]

Besides a large electrochemical window, high ionic conductivity and fast ion mobility (including the doped ions such as Li^+ for Li batteries) are the additional requirements for ILs as supporting electrolytes in high-energy devices. This means that the viscosity of ILs must be as low as possi-

[a] Dr. Z.-B. Zhou, Dr. H. Matsumoto, Dr. K. Tatsumi
Research Institute for Ubiquitous Energy Devices
National Institute of Advanced Industrial Science and Technology
1-8-31 Midorigaoka, Ikeda, Osaka 563–8577 (Japan)
Fax: (+81) 72-751-9622
E-mail: h-matsumoto@aist.go.jp

DOI: 10.1002/chem.200400817

ble and the anion involved in the ILs must have weakly coordinating ability to depress ion pairing. Therefore, the QA cation involved should be small because large ones have been found to result in high viscosities.[15–17] To date, although a large number of QA salts with a wide variety of anions have been reported,[12–33] very few of them appear to satisfy the above requirements. This is mainly due to a lack of anions, which not only have chemical and electrochemical stability but which can also form low-melting and low-viscous ILs with relatively small QA cations (total C atoms ≤ 10). For instance, several known electrochemically stable anions tend to form either high-melting (e.g. $>100\,^{\circ}C$ for high symmetry $[BF_4]^-$,[20,22,23] $[PF_6]^-$,[22,24] $[AsF_6]^-$[22]) or very highly viscous salts (e.g. >300 cP for $[BF_4]^-$,[13,25] and >1300 cP at 25 °C for large and rigid bis(oxalato)borate $[BOB]^-$[26]) with small QA cations, whereas those that can form low-melting and low-viscous ILs with small QA cations (e.g. trifluoro-*N*-(trifluoromethylsulfonyl)acetamide $[(CF_3SO_2)(CF_3CO)N]^-$,[9c,27] dicyanamide $[N(CN)_2]^-$[28]) suffer from electrochemical instability. Until recently, the development of stable, low-melting and low-viscous QA salts has been almost limited to the anion $TFSI^-$[9–13,16,29,30] because this fluoroanion not only possesses chemical and electrochemical stability[9–13,21] but it also combines low symmetry, high flexibility, and a weakly coordinating nature,[34,35] all of which are beneficial to the reduction of the cohesive forces of the salts, thus lowering the melting point and viscosity. To further explore and extend the potential applications of the QA-based ILs in electrochemical devices and other emerging research fields, such as enzyme-catalyzed reactions[30] and classic C–C formation (e.g. Heck and Suzuki coupling reactions),[36] new robust anions that can form low-melting and low-viscous ILs with small QA cations are certainly needed.

Very recently, we found that a new class of chemically and electrochemically stable and weakly coordinating fluoroanions, namely perfluoroalkyltrifluoroborates ($[R_FBF_3]^-$) (R_F = CF_3, C_2F_5, *n*-C_3F_7, *n*-C_4F_9),[37–42] can form low-melting and low-viscous ILs, even with large 1,3-dialkylimidazolium cations (<77 cP at 25 °C)[43–45] and relatively small aliphatic QA cations (58–86 cP at 25 °C).[46] More importantly, they are more resistant toward hydrolysis than their $[BF_4]^-$ analogues on account of their hydrophobicity.[43–45] Encouraged by these results, we herein report the systematic synthesis and characterization of a series of new hydrophobic and low-melting salts based on relatively small aliphatic QA cations ($[R^1R^2R^3NR]^+$, wherein R^1, R^2, R^3 = CH_3 or C_2H_5, R = *n*-C_3H_7, *n*-C_4H_9, $CH_2CH_2OCH_3$) and perfluoroalkyltrifluoroborate anions ($[R_FBF_3]^-$, R_F = CF_3, C_2F_5, *n*-C_3F_7, *n*-C_4F_9). Most of them are liquids at 25 °C, and exhibit low viscosities, moderate conductivities, and good electrochemical stability. For comparison, the corresponding QA salts with two representative anions, $[BF_4]^-$ and $TFSI^-$, were also synthesized and characterized.

Results and Discussion

Synthesis and characterization: In the present study, 36 quaternary ammonium (QA) salts, comprising the relative small QA cations $[R^1R^2R^3NR]^+$ (R^1, R^2, R^3 = CH_3 or C_2H_5, R = *n*-C_3H_7, *n*-C_4H_9, $CH_2CH_2OCH_3$) with the fluoroanions $[R_FBF_3]^-$ (R_F = CF_3, C_2F_5, *n*-C_3F_7, *n*-C_4F_9), $[BF_4]^-$, and $TFSI^-$, were synthesized according to Scheme 1. The synthesized QA salts are presented in Table 1. For convenience, a special notation for the QA cations is used (see Scheme 1): "N" denotes the QA cations and each number in the subscript denotes the number of carbons in each alkyl substituent. The subscript, "1O2", denotes the methoxyethyl ($CH_3OCH_2CH_2$) substituent.

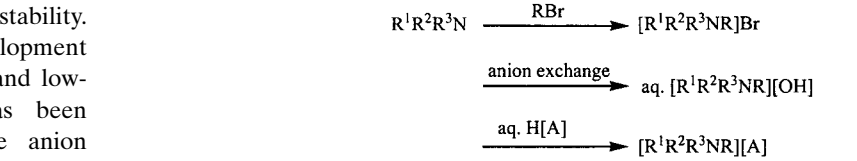

([A]⁻ = [CF3BF3]⁻, [C2F5BF3]⁻, [n-C3F7BF3]⁻, [n-C4F9BF3]⁻, [BF4]⁻, [(CF3SO2)2N]⁻)

$[R^1R^2R^3NR]^+$	R^1	R^2	R^3	R
$[N_{1223}]^+$	CH_3	C_2H_5	C_2H_5	n-C_3H_7
$[N_{1224}]^+$	CH_3	C_2H_5	C_2H_5	n-C_4H_9
$[N_{111.1O2}]^+$	CH_3	CH_3	CH_3	$CH_3OCH_2CH_2$
$[N_{112.1O2}]^+$	CH_3	CH_3	C_2H_5	$CH_3OCH_2CH_2$
$[N_{122.1O2}]^+$	CH_3	C_2H_5	C_2H_5	$CH_3OCH_2CH_2$
$[N_{222.1O2}]^+$	C_2H_5	C_2H_5	C_2H_5	$CH_3OCH_2CH_2$

Scheme 1.

ILs are usually prepared from halide salts as the source of the cation component. In this case, it is very difficult to avoid halide impurities in the resulting ILs. It is well known that the presence of halide impurities in the resultant ILs significantly alters the physicochemical properties of the ILs.[47] To depress halide contamination, the new salts $[R^1R^2R^3NR][R_FBF_3]$ in the present study were prepared via a modified route by neutralization of aqueous solutions of $[R^1R^2R^3NR][OH]$ with aqueous solutions of $H[R_FBF_3]$ (Scheme 1). The aqueous $[R^1R^2R^3NR][OH]$ salts were pro-

Table 1. Thermal properties of various prepared salts.

Entry	Salts	T_g[a] [°C]	T_c[b] [°C]	$T_{s\text{-}s}$[c] [°C]	T_m[d] [°C]	ΔS_m[e] [J mol^{-1} K^{-1}]	T_d[f] [°C]
1	$N_{1223}[CF_3BF_3]$			−40, −30, −21	95	7.4	252
2	$N_{1224}[CF_3BF_3]$			−40	−3	9.5	212
3	$N_{111.1O2}[CF_3BF_3]$			51	77	33.3	186
4	$N_{112.1O2}[CF_3BF_3]$			−7	8	28.8	163
5	$N_{122.1O2}[CF_3BF_3]$				−22	29.9	174
6	$N_{222.1O2}[CF_3BF_3]$				10	60.7	210
7	$N_{1223}[C_2F_5BF_3]$			−67, −40	54	29.3	315
8	$N_{1224}[C_2F_5BF_3]$			−49	15	32.7	320
9	$N_{111.1O2}[C_2F_5BF_3]$				30	38.4	326
10	$N_{112.1O2}[C_2F_5BF_3]$	−117	−76, −65		−33	57.9	307
11	$N_{122.1O2}[C_2F_5BF_3]$	−113					322
12	$N_{222.1O2}[C_2F_5BF_3]$	−98	-63, −51		3	88.4	345
13	$N_{1223}[n\text{-}C_3F_7BF_3]$			−53, 25	57	15.7	315
14	$N_{1224}[n\text{-}C_3F_7BF_3]$			−58	50	41.1	307
15	$N_{111.1O2}[n\text{-}C_3F_7BF_3]$			−86	23	45.9	284
16	$N_{112.1O2}[n\text{-}C_3F_7BF_3]$	−113					291
17	$N_{122.1O2}[n\text{-}C_3F_7BF_3]$	−112					275
18	$N_{222.1O2}[n\text{-}C_3F_7BF_3]$			−33	6	30.7	351
19	$N_{1223}[n\text{-}C_4F_9BF_3]$			12, 24	54	17.9	273
20	$N_{1224}[n\text{-}C_4F_9BF_3]$			−76, 3	60	29.6	314
21	$N_{111.1O2}[n\text{-}C_4F_9BF_3]$				50	54.4	307
22	$N_{112.1O2}[n\text{-}C_4F_9BF_3]$	−110	−56		−28	60.2	283
23	$N_{122.1O2}[n\text{-}C_4F_9BF_3]$	−108					287
24	$N_{222.1O2}[n\text{-}C_4F_9BF_3]$			−11	11	26.1	305
25	$N_{1223}[BF_4]$				186	13.6	393
26	$N_{1224}[BF_4]$				165	20.6	392
27	$N_{111.1O2}[BF_4]$				54[g]	45.8	376
28	$N_{112.1O2}[BF_4]$	−97[h]	−26		4[i]	55.0	377
29	$N_{122.1O2}[BF_4]$	−95	−51		8[j]	61.0	372
30	$N_{222.1O2}[BF_4]$				56	57.0	372
31	N_{1223}[TFSI]			−21, −2	14	15.8	404
32	N_{1224}[TFSI]	−93	−44		9	87.6	400
33	$N_{111.1O2}$[TFSI]				37	85.6	382
34	$N_{112.1O2}$[TFSI]	−96[k]					388
35	$N_{122.1O2}$[TFSI]	−95					390
36	$N_{222.1O2}$[TFSI]	−82	−43		20	81.3	386

[a] Glass transition temperature determined by DSC on heating. [b] Crystallization temperature determined by DSC on heating. [c] Solid–solid transition temperature determined by DSC on heating. [d] Melting point determined by DSC on heating. [e] Entropy of melting ($\Delta S_m = \Delta H_m/T_m$, where ΔH_m is melting enthalpy at T_m[K]). [f] Decomposition temperature determined by TGA. [g] 64.[19b] [h] −97;[19b] [i] 13.[19b] [j] 9.[13] [k] −93.[25]

duced by anion exchange of the corresponding $[R^1R^2R^3NR]Br$ salts, which were synthesized by reaction of trialkylamines with an equivalent of the appropriate alkyl bromide in anhydrous acetone in an autoclave. The exception was $N_{111.1O2}Br$, which was directly prepared at room temperature. Aqueous $H[R_FBF_3]$ was prepared by cation exchange of the corresponding $K[R_FBF_3]$.[38] The salts based on $[BF_4]^-$ and $TFSI^-$ were similarly prepared, except aqueous $H[BF_4]$ and aqueous H[TFSI] were used instead of aqueous $H[R_FBF_3]$. All the salts prepared by this modified method (Table 1) were found to contain less than 30 ppm of Br^- and K^+ ions, as estimated by fluorescence X-ray spectrometry. In addition, the $[R_FBF_3]^-$ and $TFSI^-$ salts are immiscible with water to some extent, and this allows these salts to be separated directly from the aqueous phase. The final yields of the prepared salts ranged from moderate to high (66–92%). In the $[R_FBF_3]^-$ series, an increase in the length of the perfluoroalkyl (R_F) chain in the $[R_FBF_3]^-$ generally resulted in an increase in the yield, as expected by the increased hydrophobicity.

The newly prepared salts in Table 1 were characterized by ^1H, ^{19}F, and ^{11}B NMR, FAB-MS, and elemental analysis. All the characterization data are consistent with the expected compositions and structures. The water content in the $[R_FBF_3]^-$ and $TFSI^-$ salts was less than 50 ppm after drying at 70 °C and 0.02 Torr for 24 h owing to their hydrophobicity, whereas the $[BF_4]^-$ salts are miscible with water and still contained an appreciable amount of water (≈400–600 ppm), even after rigorously drying at 80 °C and 0.02 Torr for 48 h. In our experience, it is rather difficult to reduce the water content any further in these hydrophilic liquids because drying at a higher temperature gives rise to a hydrolysis reaction between the $[BF_4]^-$ and the residual water.

The thermal properties of these prepared salts, including the QA bromide, were determined by differential scanning calorimetry (DSC), and thermal gravimetric analysis (TGA). For the salts that are liquids at 25 °C, the fundamental properties including density (d), dynamic viscosity (η), ionic conductivity (κ), and electrochemical stability, were also determined. Some of the characterization data are pre-

sented in Tables 1–3. The influence of the structure variation in the cation and anion on the above properties will be detailed in the following sections.

Phase transition: The solid–liquid phase transitions of these QA salts were investigated by differential scanning calorimetry (DSC). The data for the glass transition temperature (T_g), crystallization temperature (T_c), solid–solid transition (T_{s-s}), and melting point (T_m), if appropriate, are collected in Table 1. In general, four types of phase transition behavior were observed for these QA salts on heating. The typical DSC traces for these four types of behavior are exemplified in Figure 1. The first type of behavior is characterized by

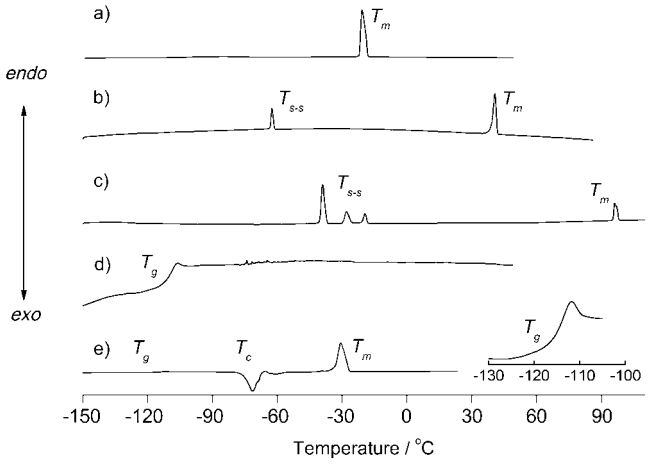

Figure 1. DSC traces on heating for a) $N_{122.1O2}[CF_3BF_3]$, b) $N_{1224}[n\text{-}C_3F_7BF_3]$, c) $N_{1223}[CF_3BF_3]$, d) $N_{122.1O2}[C_2F_5BF_3]$, and e) $N_{112.1O2}[C_2F_5BF_3]$. Inset: an enlarged trace for e) $N_{112.1O2}[C_2F_5BF_3]$ in the temperature range close to T_g.

the salts that have a single melting transition (Figure 1a, entries 5, 6, 9, 21, 25–27, 30, and 33 in Table 1). The second type of behavior is represented by a number of salts that exhibited one or multiple solid–solid transitions (T_{s-s}) before melting (Figure 1b and c, entries 1–4, 7, 8, 13–15, 18–20, 24, and 31 in Table 1). As can be seen in Table 1, most of the $[R_FBF_3]^-$ salts show this behavior; however, such behavior was not observed among the $[BF_4]^-$ salts. The unique property associated with this behavior will be detailed below. The third type of behavior is represented by the salts that only exhibited glass transitions at a very low temperature in the range −95 to −113 °C without melting (Figure 1d, entries 11, 16, 17, 23, 34, and 35 in Table 1). The fourth type of behavior was observed in the remaining salts (entries 10, 12, 22, 28, 29, 32, and 36 in Table 1). A typical DSC trace for this behavior is shown in Figure 1e. On heating, these salts showed a glass transition (T_g) at a very low temperature (from −95 to −117 °C) to form a supercooled liquid, which then crystallized (T_c, observed as an exothermic peak) at a relatively high temperature, followed by a melting transition (T_m) as the temperature increased further.

The melting entropies (ΔS_m) of the prepared salts are also presented in Table 1. Timmermans[48] reported that plastic crystal phases in simple molecular compounds typically have a $\Delta S_m < 20\,J\,K^{-1}\,mol^{-1}$. Recently, MacFarlane[29] and coworkers reported that it is more appropriate to modify this criterion to $\approx 40\,J\,K^{-1}\,mol^{-1}$ when a relative large and flexible anion (e.g. $TFSI^-$) exists in the ionic compound. This new criterion appears to be applicable to the $[R_FBF_3]^-$ salts (R_F = CF_3, C_2F_5, n-C_3F_7, n-C_4F_9), as these new anions containing a perfluoroalkyl (R_F) chain may have higher degrees of freedom than those with simple symmetry (e.g. $[BF_4]^-$[23] and $[PF_6]^-$[24]), and the salts with the former anions, therefore, may afford higher residual entropies of melting than those with the latter anions. Thus, it seems reasonable that many of the $[R_FBF_3]^-$ salts, which show solid–solid transitions with a $\Delta S_m < 40\,J\,K^{-1}\,mol^{-1}$ (Table 1), are exhibiting varying extents of plastic crystal behavior. It is of current interest to explore conductive organic plastic crystals as an all-solid-state electrolyte for high-energy devices, such as Li batteries.[49,50] Therefore, our future work will investigate the conductivity behavior of these salts and mixtures with their corresponding lithium salts. Among the salts to be investigated, $N_{1223}[CF_3BF_3]$ (entry 1) and $N_{1223}[C_2F_5BF_3]$ (entry 7) may be the particularly interesting ones that enter a plastic crystal phase at a low temperature (≈−40 °C for entry 7 and ≈−21 °C for entry 1) and exist in this phase up to a high temperature (95 °C for entry 1 and 54 °C for entry 7) before melting. The plastic crystal phase within these temperature regions is very suitable for practical applications because the electrolytes in many electrochemical devices are required to operate in an ambient temperature range (from −40 to 80 °C).

Melting point: It was reported that the melting point (T_m) of a compound is determined by the strength of its crystal lattice, which in turn is controlled by three main factors: intermolecular forces, molecular symmetry, and the conformational degrees of the freedom of a molecule.[51] For aliphatic QA salts, the influence of structure variation in the cation and anion on the T_m has been investigated previously.[15–17,22–24,27–29,31] Generally, low symmetry and a relatively large size of the cation combined with low symmetry and effective charge distribution in the anion favor destabilization of the packing efficiency in the crystal lattice of the QA salts, thus decreasing the strength of the crystal lattice which in turn lowers the T_m. Additionally, introducing an alkyl ether to the QA cation also tends to depress the T_m in some cases.[9,19,25,26]

Therefore, on the basis of this knowledge, we tried to prepare low-melting QA salts from QA cations with relatively low symmetry and/or having an alkyl ether substituent, as shown in Scheme 1. Indeed, low melting points were achieved for most of the salts in our study (Table 1). With the exceptions of $N_{1223}[BF_4]$ and $N_{1224}[BF_4]$, all the prepared salts have a T_m of < 100 °C, 23 are liquids at room temperature, most of the liquids are those containing an alkyl ether ($CH_3OCH_2CH_2$) substituent in the cation.

Figure 2 shows the observed T_m of these salts. As a general trend, for each anion, the salts with cations of higher sym-

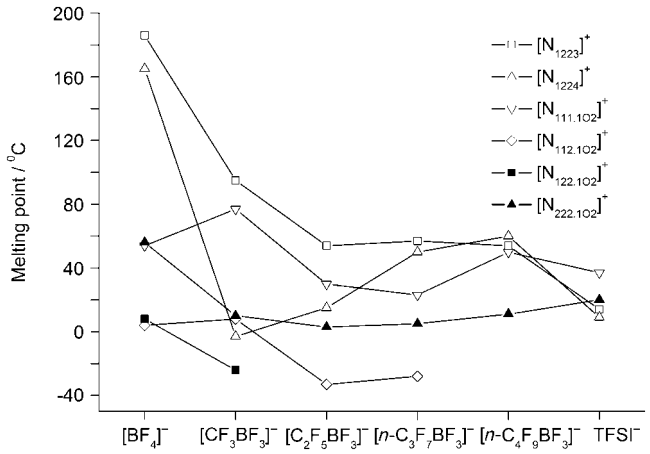

Figure 2. Melting point of various salts.

metry show a higher T_m than those with cations of lower symmetry. For example, the $[N_{2222}]^+$ salts with $[R_FBF_3]^-$ (R_F = C_2F_5, n-C_3F_7, n-C_4F_9) decompose directly at a high temperature (278–290 °C) instead of melting;[38] however, replacing the $[N_{2222}]^+$ of these salts with $[N_{1223}]^+$, which has a lower symmetry but the same formula weight, lowers the T_m to the low-melting range (54–97 °C). This is also true for the TFSI salts. For example, N_{2222}[TFSI] (105–109 °C)[16,17] versus N_{1223}[TFSI] (14 °C). Likewise, the salts with lower symmetry $[N_{112.1O2}]^+$ and $[N_{122.1O2}]^+$ (containing three different substituents) generally exhibit a lower T_m than the corresponding salts with higher symmetry $[N_{111.1O2}]^+$ and $[N_{222.1O2}]^+$ (containing two different substituents). Exchanging the $[N_{1223}]^+$ of the salts for the larger $[N_{1224}]^+$ generally gave rise to a further decrease of the T_m (e.g. entry 1 versus 2, 7 versus 8, 13 versus 14, 25 versus 26, 31 versus 32 in Table 1). Likewise, for the same cation, all the salts with lower symmetry, $[R_FBF_3]^-$ and $TFSI^-$, exhibit a lower T_m than those with higher symmetry $[BF_4]^-$.

Another notable effect on the T_m of the aliphatic QA salt is to introduce a methoxyethyl ($CH_3OCH_2CH_2$) group to the QA cation, which was also observed in other publications.[19,25,26] However, the reasons for this effect are not well understood. To gain an insight into the influence of the alkyl ether chain on the T_m of the aliphatic QA salt, we therefore carried out a comparative study of the T_m of the $[N_{1224}]^+$ salts with those of the $[N_{122.1O2}]^+$ salts. As shown in Figure 2, for all the $[N_{1224}]^+$ salts, replacing the n-butyl group in the $[N_{1224}]^+$ with an isoelectronic methoxyethyl ($CH_3OCH_2CH_2$) group resulted in a significant decrease in the T_m in all cases. For example, $N_{122.1O2}$[BF_4] (8 °C) versus N_{1224}[BF_4] (165 °C), $N_{122.1O2}$[CF_3BF_3] (−22 °C) versus N_{1224}[CF_3BF_3] (−3 °C), and only T_g (−95 to −113 °C) for the $[N_{122.1O2}]^+$ salts with $[R_FBF_3]^-$ (R_F = C_2F_5, n-C_3F_7, n-C_4F_9, entries 11, 17, and 23) and $TFSI^-$ (entry 35). In addition, the salts with the cations $[N_{111.1O2}]^+$, $[N_{112.1O2}]^+$, and $[N_{222.1O2}]^+$ also show a low T_m. Moreover, low-melting events have also been observed in the QA salts containing other alkyl ether groups, such as methoxymethyl (CH_3OCH_2), ethoxymethyl ($CH_3CH_2OCH_2$), and ethoxyethyl ($CH_3CH_2OCH_2CH_2$).[9,19,25,26] Given that the alkyl ether group is more flexible but more polar than its isoelectronic alkyl group, and the flexibility tends to lower the T_m, whereas the polarity has an opposite effect, a tentative explanation for the lower T_m for the QA salts containing an alkyl ether group is that the better flexibility of the alkyl ether group might prevail over its polarity and thus plays a decisive role in determining the T_m.

Glass transition: Figure 3 shows the glass transition temperature (T_g) of the salts in Table 1. It appears that the T_g of these QA salts is mainly governed by the strength of ion in-

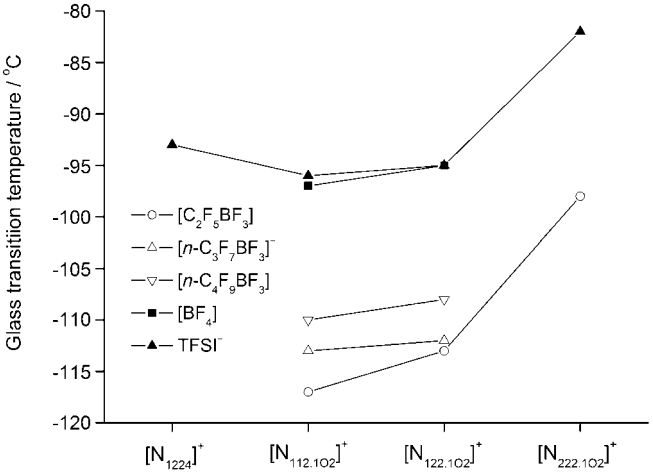

Figure 3. Glass transition temperature of various ionic liquids.

teractions, the ion size, as well as the flexibility and polarizability of the anion. As seen in Figure 3, the T_g of the salts with large $[R_FBF_3]^-$ (−117 to −98 °C, R_F = C_2F_5, n-C_3F_7, n-C_4F_9) are all lower than those with the small $[BF_4]^-$ (−97 °C for entry 28 and −95 °C for entry 29) or the large, but a little polarizable $TFSI^-$ (−82 to −96 °C), and much lower than those with the large nonfluorinated and more rigid and polarizable $[BOB]^-$ (it comprises two rigid five-member rings and each of them contains two carbonyl (C=O) groups, T_g = −36 to −44 °C).[26]

For the same cation, the T_g regularly increases in the order $[C_2F_5BF_3]^- < [n\text{-}C_3F_7BF_3]^- < [n\text{-}C_4F_9BF_3]^- < [BF_4]^- \approx TFSI^- \ll [BOB]^-$. A similar trend was also observed in the related imidazolium salts.[44,45] This trend strongly suggests that 1) replacing the $[BF_4]^-$ with a larger $[R_FBF_3]^-$ weakens the electrostatic interactions (including possible hydrogen bonding) between the cation and anion in the salt, which in turn decreases the T_g, 2) the decrease of the electrostatic interactions dominates over the increase of van der Waals interactions in the $[R_FBF_3]^-$ salts (R_F = C_2F_5, n-C_3F_7, n-C_4F_9) owing to the extremely low polarizability of fluorine atom, and 3) the ion interactions in the salts with the small $[BF_4]^-$ are influenced by the electrostatic interactions to a greater extent than by van der Waals interactions, while those in the

$[R_FBF_3]^-$ salts (R_F = C_2F_5, n-C_3F_7, n-C_4F_9) are more under the control of van der Waals interactions rather than electrostatic interactions because the T_g increased as the size of the $[R_FBF_3]^-$ increased.

On the other hand, one may note that the $TFSI^-$ salts show a slightly higher T_g than the corresponding $[BF_4]^-$ salts, and a much higher T_g than the corresponding $[R_FBF_3]^-$ salts (Figure 3 and Table 1), although the $TFSI^-$ has a much better flexibility and charge distribution than the $[BF_4]^-$ salts and would be expected to give a lower T_g for the corresponding salts. This result may be attributed to 1) the size of the $TFSI^-$ is much larger than that of the $[BF_4]^-$, and 2) the partially fluorinated $TFSI^-$ (it contains two sulfonyl (-SO_2-) groups) is more polarizable than the perfluorinated $[BF_4]^-$ and highly perfluorinated $[R_FBF_3]^-$, both of which significantly trade off the flexibility and charge distribution of the $TFSI^-$ and tend to increase the attractive forces (i.e. van der Waals interactions) in the $TFSI^-$ salts, thus raising the T_g. Moreover, comparing the T_g of the nonfluorinated $[BOB]^-$ salts with that of the perfluorinated $[n\text{-}C_4F_9BF_3]^-$ salts (the size of the $[n\text{-}C_4F_9BF_3]^-$ should be larger than that of the $[BOB]^-$ viz. $[B(C_2O_4)]^-$) more clearly manifests the significant impact of rigidity and polarizability of the anion, for example, $N_{112.1O2}[BOB]$ (−36 °C)[26] versus $N_{112.1O2}[n\text{-}C_4F_9BF_3]$ (−110 °C).

For the same anion, the T_g value of all the salts increased as the cation size increased, as expected by the increased van der Waals interactions. Because the glass transition temperature (T_g) is a qualitative signature of ion mobility in ILs and a low T_g is a sign of high ion mobility,[16b,25,26] the lower T_g of the $[R_FBF_3]^-$ salts compared to that of the $[BF_4]^-$ salts may partly explain why the former exhibit lower viscosities than the latter (see the viscosity section below).

Thermogravimetric analysis: The thermal stability of the salts was determined by TGA. Figure 4 shows the decomposition temperature (T_d) of the QA salts in Table 1. As shown in Figure 4, the salts containing $TFSI^-$ and $[BF_4]^-$ are more stable than those containing $[R_FBF_3]^-$, irrespective of the cations, and the thermal stability of these salts generally increases in the order $[CF_3BF_3]^- < [n\text{-}C_3F_7BF_3]^- \approx [n\text{-}C_4F_9BF_3]^- \approx [C_2F_5BF_3]^- < [BF_4]^- \approx TFSI^-$. This trend indicates that the anion has a significant impact on the thermal stability of the QA salts, as observed in the imidazolium salts with these anions.[45] Figure 5 displays thermogravimetric traces of six $[N_{1224}]^+$ salts with different anions as examples to illustrate the different decomposition behavior of these salts during pyrolysis. The thermal stability order and decomposition behavior of these QA salts with $[R_FBF_3]^-$ is concurrent with our recent observations with the corresponding imidazolium salts.[45] The lower thermal stability of the $[R_FBF_3]^-$ salts, relative to those containing $[BF_4]^-$ and $TFSI^-$, is essentially attributed to the pyrolysis of $[R_FBF_3]^-$ at a low temperature.[45] We will now describe the decomposition of the $N_{1224}[CF_3BF_3]$ in detail, as exemplified by the family of $[R_FBF_3]^-$ salts. As seen in Figure 5, $N_{1224}[CF_3BF_3]$ exhibited a distinct two-stage decomposition behavior, as observed in the related imidazolium salts.[45] It started to decompose at ≈200 °C, and ≈18 % of the weight loss was observed up to 300 °C, which corresponds to the elimination of a CF_2 moiety from this salt, most probably $[CF_3BF_3]^- \rightarrow [BF_4]^-$ + other products (formed from CF_2 carbene). Subsequently, the weight of the residue remained almost constant until ≈380 °C. It began to decompose again above ≈390 °C, and the subsequent decomposition behavior of the residue was exactly in agreement with that of $N_{1224}[BF_4]$. Similar decomposition behavior was also observed in the other QA salts with $[CF_3BF_3]^-$. These results strongly indicate that decomposition of the $[CF_3BF_3]^-$ salts is initiated from the pyrolysis of $[CF_3BF_3]^-$.

For a constant anion, it seems that the variation in the QA cation has less effect on the thermal stability of the corresponding salts, with the exception of the $[CF_3BF_3]^-$ series, where the salts containing the methoxyethyl group in the

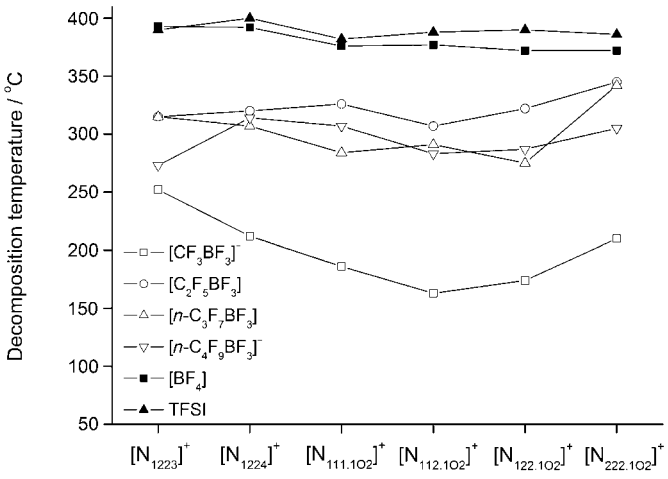

Figure 4. Thermal stability of various ionic liquids.

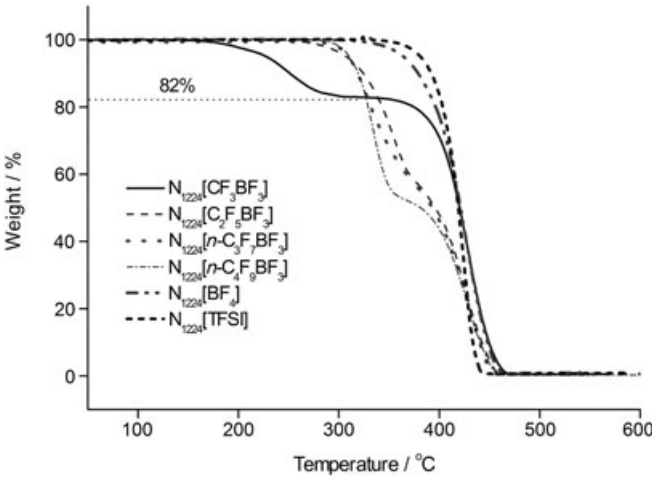

Figure 5. TGA traces of the $[N_{1224}]^+$ salts with $[R_FBF_3]^-$ (R_F = CF_3, C_2F_5, n-C_3F_7, n-C_4F_9), $[BF_4]^-$, and $TFSI^-$.

QA cation show less thermal stability than their tetraalkylammonium analogues, as shown in Figure 4.

Density: Figure 6 shows the densities of the liquid QA salts based on the $[R_FBF_3]^-$ (R_F = CF_3, C_2F_5, n-C_3F_7, n-C_4F_9), $[BF_4]^-$, and $TFSI^-$ at 25 °C. The density (d) lies in the range

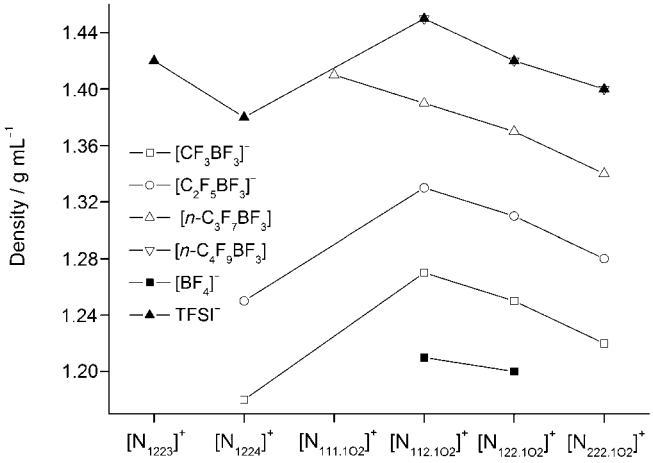

Figure 6. Density of various liquid salts at 25 °C.

1.16–1.55 g mL^{-1}. Because a number of the liquid salts have a methoxyethyl ($CH_3OCH_2CH_2$) group in their cation, the density trend is more noticeable for these salts. As seen in Figure 6, for a given anion, the densities of the trialkyl(2-methoxyethyl)ammonium salts decreased when the formula weight (M_w) of the cation increased. The densities of the trialkyl(2-methoxyethyl)ammonium salts are a little higher than those of the $[N_{1224}]^+$ salts with the same anion. For example, keeping the $[C_2F_5BF_3]^-$ constant, the density falls in the order 9 ($[N_{111.1O2}]^+$) > 10 ($[N_{112.1O2}]^+$) > 11 ($[N_{122.1O2}]^+$) > 12 ($[N_{222.1O2}]^+$) > 8 ($[N_{1224}]^+$).

On the other hand, for a given cation, the density gradually increased as the bulkiness of the fluoroanion increased in the order $[BF_4]^- < [CF_3BF_3]^- < [C_2F_5BF_3]^- < [n\text{-}C_3F_7BF_3]^- < [n\text{-}C_4F_9BF_3]^- \approx TFSI^-$. This trend is consistent with our recent results for the related imidazolium ILs.[45] Moreover, as shown in Figure 5, in the family of the trialkyl(2-methoxyethyl)ammonium ($[N_{xyz.1O2}]^+$) with $[C_nF_{2n+1}BF_3]^-$ (n = 0–4), it seems that the density decreased linearly with increasing number of CH_2 units in the $[N_{xyz.1O2}]^+$, and linearly increased with increasing the number of CF_2 units in the $[C_nF_{2n+1}BF_3]^-$ (n = 0–4). By a simple regression analysis, the densities of these 15 liquids can be expressed linearly [Eq. (1)], for m = 6–9, n = 0–4; r^2 = 0.998, where m and n represent the number of carbon atoms in the cation and anion, respectively.

$$d\ (\mathrm{g\,mL^{-1}}) = 1.38 - 0.024\,m + 0.058\,n \qquad (1)$$

Viscosity: The viscosity of the QA salts is essentially determined by the strength of ion interactions (mainly including the electrostatic and van der Waals interactions), ion size, and by the polarizability and flexibility of the anion. Figure 7 shows the viscosities (η) of the liquid salts based on the $[R_FBF_3]^-$ (R_F = CF_3, C_2F_5, n-C_3F_7, n-C_4F_9), $[BF_4]^-$, and $TFSI^-$ (Table 2) at 25 °C. The viscosities of the $[R_FBF_3]^-$ and

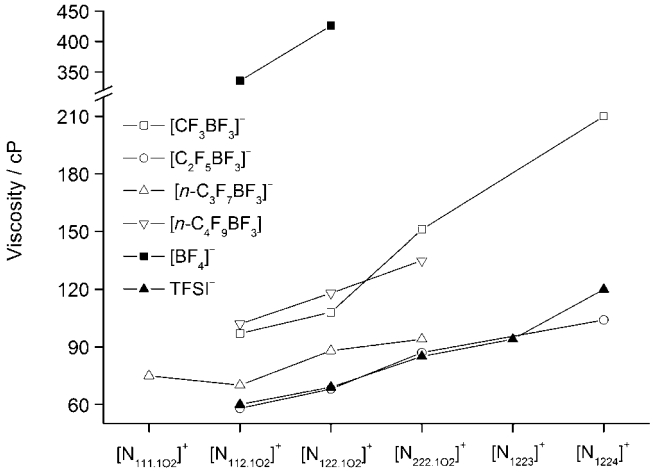

Figure 7. Viscosity of various liquid salts at 25 °C.

Table 2. Density, viscosity, and specific conductivity of liquid salts at 25 °C (water content: < 50 ppm in $[R_FBF_4]^-$ and $TFSI^-$ salts, and 400–600 ppm in the $[BF_4]^-$ salts).

Entry[a]	Salts	d[b] [g mL^{-1}]	η[c] [cP]	κ[d] [mS cm^{-1}]
2	$N_{1224}[CF_3BF_3]$	1.18	210	2.1
4	$N_{112.1O2}[CF_3BF_3]$	1.27	97	2.5
5	$N_{122.1O2}[CF_3BF_3]$	1.25	108	3.0
6	$N_{222.1O2}[CF_3BF_3]$	1.22	151	2.0
8	$N_{1224}[C_2F_5BF_3]$	1.25	104	2.3
10	$N_{112.1O2}[C_2F_5BF_3]$	1.33	58	3.8
11	$N_{122.1O2}[C_2F_5BF_3]$	1.31	68	3.2
12	$N_{222.1O2}[C_2F_5BF_3]$	1.28	87	2.4
15	$N_{111.1O2}[n\text{-}C_3F_7BF_3]$	1.41	76	2.5
16	$N_{112.1O2}[n\text{-}C_3F_7BF_3]$	1.39	70	2.6
17	$N_{122.1O2}[n\text{-}C_3F_7BF_3]$	1.37	88	1.9
18	$N_{222.1O2}[n\text{-}C_3F_7BF_3]$	1.34	91	1.8
22	$N_{112.1O2}[n\text{-}C_4F_9BF_3]$	1.45	102	1.5
23	$N_{122.1O2}[n\text{-}C_4F_9BF_3]$	1.42	118	1.3
24	$N_{222.1O2}[n\text{-}C_4F_9BF_3]$	1.40	135	1.1
28	$N_{112.1O2}[BF_4]$	1.21	335[e]	1.7[f]
29	$N_{122.1O2}[BF_4]$	1.20	426	1.3
31	N_{1223}[TFSI]	1.42	94	2.2
32	N_{1224}[TFSI]	1.38	120	1.6
34	$N_{112.1O2}$[TFSI]	1.45	60	3.1
35	$N_{122.1O2}$[TFSI]	1.42	69	2.6
36	$N_{222.1O2}$[TFSI]	1.40	85	2.1

[a] In accord with the entries in Table 1. [b] Density. [c] Viscosity. [d] Specific conductivity. [e] 1.7.[25] [f] ≈335.[25]

$TFSI^-$ series of ILs are in the range 58–210 cP, all of which are significantly lower by > 100 cP than those of the $[BF_4]^-$ salts (335 cP for entry 28 and 426 cP for entry 29 at 25 °C), and much lower than those of the QA salts with the non-fluorinated $[BOB]^-$ (> 1300 cP at 25 °C[26]).

The lower viscosities for the $[R_FBF_3]^-$ and $TFSI^-$ ILs than those of the $[BF_4]^-$ salts may be explained by the decreased ion interactions and increased ion mobility owing to improved charge distribution, lower symmetry, and lower polarizability for the $[R_FBF_3]^-$ salts, and to improved charge distribution, larger flexibility, and lower symmetry for the $TFSI^-$ salts. Notwithstanding that the $[BOB]^-$ is among the most weakly coordinating anions,[53] the extremely high viscosities were observed for all $[BOB]^-$ salts,[26] which is essentially attributed to high rigidity (comprising two five-membered rings) and some polarizability (containing four carbonyl (C=O) groups) and large size of the $[BOB]^-$, as discussed for the T_g. The first factor reduces the flexibility and the latter two ones increase the van der Waals interactions in the salts, all of which in turn significantly increase the viscosity. These impressive examples based on the $[BOB]^-$ and its derivatives clearly indicate that an anion with high rigidity and polarizability and large size is not suitable for forming low-viscous ILs, despite its weakly coordinating ability.[26]

In the family of the fluoroborate ($[R_FBF_3]^-$ and $[BF_4]^-$) ILs, for a given cation, the viscosities show the increasing order $[C_2F_5BF_3]^- < [n\text{-}C_3F_7BF_3]^- < [CF_3BF_3]^- < [n\text{-}C_4F_9BF_3]^- \ll [BF_4]^-$, with the exception of $N_{222.1O2}[CF_3BF_3]$. It is very interesting to note that this order of viscosity is exactly consistent with that of the T_g (i.e. the lower the T_g, the more fluid the ILs), with the exception of the salts containing the $[CF_3BF_3]^-$ (no T_g observed). These results further suggest that the ion interactions in the salts with relative large $[R_FBF_3]^-$ (R_F = C_2F_5, n-C_3F_7, n-C_4F_9) are essentially determined by van der Waals interactions, and a very large anion in this class (e.g. $[n\text{-}C_4F_9BF_3]^-$) is therefore unsuitable for forming low-viscous ILs, despite its good charge distribution and extremely low polarizability. The most unexpected result is that the salts with the smaller $[CF_3BF_3]^-$ show a higher viscosity than those with the larger $[R_FBF_3]^-$ (R_F = C_2F_5, n-C_3F_7). It appears that 1) ion interactions in the former are stronger than those in the latter and are still under the influence of the electrostatic interactions owing to the small size of the $[CF_3BF_3]^-$, as in the case of the $[BF_4]^-$ salts; and 2) the $[R_FBF_3]^-$ with a longer R_F group (R_F = C_2F_5, n-C_3F_7) have more degrees of freedom than the $[CF_3BF_3]^-$, thus lowering the viscosity. The lowest viscosities for the $[C_2F_5BF_3]^-$ salts are essentially attributed to a good charge distribution and medium size for the $[C_2F_5BF_3]^-$.

As shown in Figure 7, for the same cation, the viscosity values of the $TFSI^-$ salts are nearly equivalent to those of the most fluid $[C_2F_5BF_3]^-$ series (e.g. $N_{112.1O2}[TFSI]$ (60 cP) versus $N_{112.1O2}[C_2F_5BF_3]$ (58 cP) and $N_{122.1O2}[TFSI]$ (69 cP) versus $N_{122.1O2}[C_2F_5BF_3]$ (68 cP)), although the $[TFSI]^-$ has a larger size than the $[C_2F_5BF_3]^-$. It seems that improved flexibility and charge delocalization of the $[TFSI]^-$ plays a dominant role over its size and polarizability in determining the viscosity. All the above results indicate that the viscosities of the QA salts are strongly dependent on the type of anion present. Therefore, in the search of more low-viscous QA salts, new stable anions, especially fluoroanions with relatively low symmetry, high flexibility, and good charge distribution, are expected to be discovered and investigated in future.

The structure variation in the cation also influences the viscosity. For the same anion, the viscosities of the QA salts containing a methoxyethyl ($CH_3OCH_2CH_2$) group are generally lower than those of the tetraalkylammonium salts (e.g. entries 9–12 versus 8). This may be attributable to having a flexible methoxyethyl group in the QA cation that results in an increase in the ion mobility, as the T_g of the former group of salts is lower than that of the latter one (Figure 3). In the family of QA salts containing a methoxyethyl group, the viscosity increased as the cation size increased in the order $[N_{112.1O2}]^+$, $[N_{111.1O2}]^+ < [N_{122.1O2}]^+ < [N_{222.1O2}]^+$, as expected by the increase of van der Waals interactions. This trend suggests that, to reduce the viscosity of the QA salts further, the cation involved should be smaller, or at least not larger, than those used in this study.

It should be noted that the viscosities of all the QA salts in the present study are all remarkably higher than those of the related 1,3-dialkylimidazolium salts with a similar formula weight.[43–45] For example, the viscosity of the $N_{112.1O2}[CF_3BF_3]$ (M_w 269) is 97 cP at 25 °C, which is ≈ 1.3 times greater than that of the 1-methyl-2-methoxyethylimidazolium salt with $[CF_3BF_3]^-$ (43 cP at 25 °C, M_w 278).[44,45] It seems that the almost flat shape and good charge distribution of the imidazolium ring plays a critical role in lowering the viscosity. This may explain why the five-membered cyclic QA cations, *N*-alkyl-*N*-methylpyrrolidinium, are preferred to the acyclic QA cations to form ILs in recent studies.[11,12,29] The reason is that the former cations show a quasiflat shape to some extent and can form more fluid ILs than acyclic QA cations containing the same number of carbon atoms, for example, $P_{13}[TFSI]$ ($[P_{13}]^+$ *N*-methyl-*N*-propylpyrrolidinium, 63 cP at 25 °C) versus $N_{1124}[TFSI]$ (110 cP at 25 °C).[16c] Therefore, it seems reasonable that $[R_FBF_3]^-$ could form low-viscous ILs with the pyrrolidinium cations.

Conductivity: It appears that the ionic conductivities of these QA salts are mainly governed by their viscosities and formula weight. Figure 8 shows the specific conductivities (κ) of the liquid salts based on the $[R_FBF_3]^-$ (R_F = CF_3, C_2F_5, n-C_3F_7, n-C_4F_9), $[BF_4]^-$, and $TFSI^-$ at 25 °C (Table 2). For a given anion, the conductivity values decreased in the order $[N_{112.1O2}]^+ > [N_{122.1O2}]^+ > N_{1223}$, $[N_{222.1O2}]^+ > [N_{1224}]^+$ with the exception of the $N_{122.1O2}[CF_3BF_3]$, as expected by the increased viscosity (Figure 7), and formula weight because the number of the ion carriers per unit volume generally decreased with increasing formula weight. For a given cation, the conductivity decreased in the order $[C_2F_5BF_3]^- > TFSI^-$, $[n\text{-}C_3F_7BF_3]^-$, $[CF_3BF_3]^- > [n\text{-}C_4F_9BF_3]^- \approx [BF_4]^-$. This trend strongly indicates that an anion, which has a large formula weight (e.g. $TFSI^-$, $[n\text{-}C_4F_9BF_3]^-$) or results in high viscosity (e.g. $[BF_4]^-$, $[CF_3BF_3]^-$), is unfavorable for producing highly conductive ILs. Among these QA salts, the $N_{112.1O2}[C_2F_5BF_3]$ (entry 10) exhibits the highest conductivity

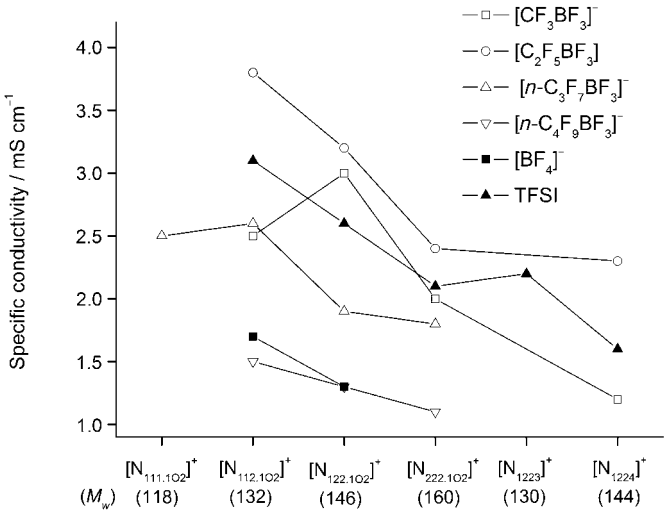

Figure 8. Specific conductivity of various liquid salts at 25 °C; the data in parentheses is formula weight (M_w) of the cation.

(3.8 mS cm^{-1} at 25 °C) because it has the lowest viscosity (58 cP at 25 °C) and a relatively low formula weight.

On the other hand, all the QA salts in this study show much lower conductivities than the imidazolium salts with a similar formula weight, for example, the most conductive QA salt $N_{112.1O2}[C_2F_5BF_3]$ (3.8 mS cm^{-1} and 57 cP at 25 °C, M_w 319) versus the 1-methyl-2-methoxyethylimidazolium salt with $[C_2F_5BF_3]^-$[45] (6.1 mS cm^{-1} and 38 cP at 25 °C, M_w 328). This is mainly caused by the higher viscosities for the former (57 cP at 25 °C) than for the latter[45] (38 cP at 25 °C). Therefore, one of the significant challenges in developing conductive QA salts is how to reduce their viscosity even further.

Electrochemical stability: The electrochemical stability of most QA salts was investigated by linear sweep voltammetry (LSV) on a glassy carbon electrode under the same conditions. The cathodic and anodic limits ($E_{cathodic}$ and E_{anodic} (V) versus ferrocene (Fc)/ferrocenium (Fc^+) redox couple) were arbitrarily defined as the potential at which the current density reached 1 mA cm^{-2} in the first scan and *IR* drop (i.e. a voltage drop associated with the electrical resistance of the electrolyte) was negligible on account of moderate conductivities. The respective $E_{cathodic}$ and E_{anodic} and electrochemical windows (ΔE (V) = $E_{anodic} - E_{cathodic}$) for these QA salts are summarized in Table 3, including previously reported values for $N_{1114}[TFSI]$[9b,16c] and $[C_2mmi][CF_3BF_3]$ ($[C_2mim]^+$ = 1-ethyl-3-methylimidazolium)[44,45]. Figure 9 displays the polarization curves of seven salts, which mainly manifests the impact of the cation structure on the $E_{cathodic}$ (i.e. the significant influence of having a methoxyethyl group in the QA cations and the sizes of these cations on the cathodic stability).

In general, the cathodic stability of the QA salts with electrochemically stable anions, such as $[BF_4]^-$, $TFSI^-$, and $[PF_6]^-$, is essentially limited by the decomposition of the QA cation. The tetraalkylammonium cations show almost the same cathodic stability, irrespective of the alkyl substituents in the cation.[20,21] These are also the cases for our QA salts. For example, the two tetraalkylammonium cations, $[N_{1114}]^+$ and $[N_{1224}]^+$, show nearly the same $E_{cathodic}$ value ($\approx$ −3.4 V). For the same cation, the $E_{cathodic}$ values of the QA salts were little affected by the anion species, for example, all the $[N_{122.1O2}]^+$ salts with various anions ($[R_FBF_3]^-$, $[BF_4]^-$, and $TFSI^-$) show a nearly equivalent $E_{cathodic}$ value (−3.3 to −3.4 V). However, the cathodic stability of the salts in this study is highly dependent on the nature of the cations, as indicated by their different $E_{cathodic}$ values

Table 3. Cathodic and anodic limits ($E_{cathodic}$ and E_{anodic} versus Fc^+/Fc at 1 mA cm^{-2}) and electrochemical windows (ΔE) for various ionic liquids determined on a glassy carbon electrode.

Salts	$E_{cathodic}$ [V]	E_{anodic} [V]	ΔE [V]
$N_{1114}[TFSI]$	−3.35	2.50	5.85
$N_{1224}[CF_3BF_3]$	−3.43	2.32	5.75
$N_{1224}[C_2F_5BF_3]$	−3.43	2.21	5.64
$N_{1224}[TFSI]$	−3.44	2.25	5.69
$N_{111.1O2}[n\text{-}C_3F_7BF_3]$	−2.75	2.24	4.99
$N_{111.1O2}[TFSI]$[a]	−2.71	2.36	5.07
$N_{112.1O2}[CF_3BF_3]$	−2.95	2.21	5.16
$N_{112.1O2}[TFSI]$	−3.13	2.35	5.48
$N_{122.1O2}[CF_3BF_3]$	−3.38	2.32	5.70
$N_{122.1O2}[C_2F_5BF_3]$	−3.32	2.29	5.61
$N_{122.1O2}[n\text{-}C_3F_7BF_3]$	−3.33	2.28	5.61
$N_{122.1O2}[n\text{-}C_4F_9BF_3]$	−3.44	2.21	5.65
$N_{122.1O2}[BF_4]$	−3.40	2.24	5.63
$N_{122.1O2}[TFSI]$	−3.33	2.34	5.67
$N_{222.1O2}[CF_3BF_3]$	−3.41	2.29	5.70
$N_{222.1O2}[C_2F_5BF_3]$	−3.41	2.22	5.63
$N_{222.1O2}[TFSI]$	−3.44	2.29	5.73
$[C_2mmi][CF_3BF_3]$	−2.49	2.14	4.63

[a] Melted at 35 °C and determined at room temperature (supercooled).

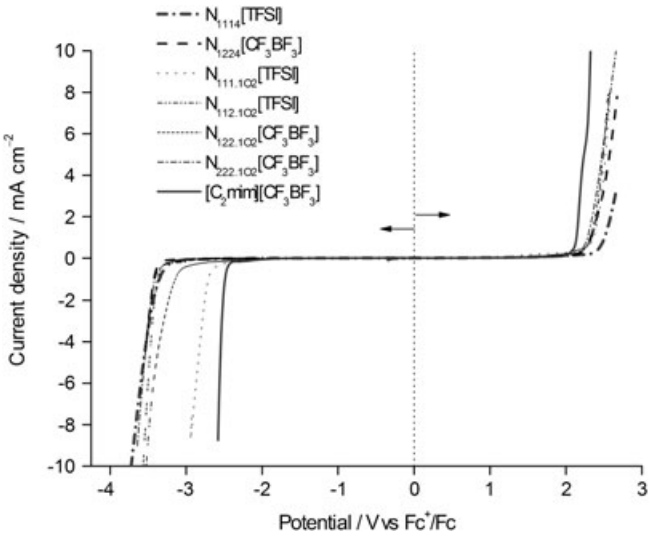

Figure 9. Linear sweep voltammogram of various ionic liquids on a glassy carbon electrode (surface area: 7.85×10^{-3} cm^{-2}) in the first scan at 25 °C; scan rate: 50 mV s^{-1}; counterelectrode: Pt wire; potential (V) was referred to ferrocene (Fc)/ferrocenium (Fc^+) redox couple in each salt; the data for $[C_2mim][CF_3BF_3]$ ($[C_2mim]^+$ = 1-ethyl-3-methylimidazolium) were obtained from the literature.[44–45]

(Table 3 and Figure 9). All the QA cations exhibit better cathodic stability than the $[C_2mim]^+$ in the following order (Table 3): $[C_2mim]^+$ (≈ -2.5 V) < $[N_{111,1O2}]^+$ (≈ -2.7 to -2.8 V) < $[N_{112,1O2}]^+$ (≈ -3.0 to -3.1 V) < $[N_{122,1O2}]^+$ (≈ -3.3 to -3.4 V) < $[N_{1114}]^+$ (≈ -3.4 V) $\approx [N_{222,1O2}]^+$ $\approx [N_{1224}]^+$ (≈ -3.4 V). This order clearly indicates that replacing the alkyl in the tetraalkylammonium cations with an isoelectronic alkyl ether tends to reduce the cathodic stability of the cations, which is more pronounced for the small cations, for example, $[N_{1114}]^+$ (≈ -3.4 V) versus $[N_{111,1O2}]^+$ (≈ -2.7 to -2.8 V), whereas increasing the sizes of trialkyl(methoxyethyl)ammonium cations tends to increase their cathodic stability, as indicated by the increased $E_{cathodic}$ values. A preliminary explanation for these results is that there are some electrostatic interactions occurring between the lone-pair electrons of oxygen atom of the methoxyethyl group and positive charge nitrogen atom in the cation, which probably increases the cathodic stability of the positively charged nitrogen atom through decreasing positive charge density on the nitrogen atom; however, it reduces the cathodic stability of the methoxyethyl group owing to a decrease of electron density on its oxygen atom. These interactions are stronger for the smaller trialkyl(methoxyethyl)ammonium on account of its higher charge density. Thus, the lower cathodic stability for the small trialkyl(methoxyethyl)ammonium cations may be caused by electroreduction of the methoxyethyl group in the cation at a relative high potential, while increasing the trialkyl(methoxyethyl)ammonium size may effectively "bury" the positive charge on the nitrogen atom of the ammonium, which in turn decreases the interactions mentioned above, thus inhibiting the decomposition of the methoxyethyl group (i.e. increasing the cathodic stability of the cation), as indicated by the highest $E_{cathodic}$ values for the $[N_{222,1O2}]^+$. These explanations have some support from results reported by Aurbach and co-workers,[53] in which the authors have identified that the electroreduction of the $N_{4444}[ClO_4]$ solutions of ether solvents, such as DME ($CH_3OCH_2CH_2OCH_3$) and THF, was essentially associated with the decomposition of the $[N_{4444}]^+$; however, addition of Li^+ ions to this electrolyte caused the electroreduction of DME and THF to precede that of the $[N_{4444}]^+$ owing to the pronounced interactions between the small Li^+ and the ether solvents. From these results, we may conclude that having an alkyl ether chain in the small QA cations is unfavorable for producing electrochemically stable QA salts. The distinctive cathodic stability of the tetraalkylammoniums (e.g. $[N_{1114}]^+$ and $[N_{1224}]^+$) and large trialkyl(methoxyethyl)-ammonium (e.g. $[N_{222,1O2}]^+$) may favor their salts with electrochemically stable anions as promising candidates for electrolytes in high-energy devices.

For anodic stability, as shown in Figure 9 and Table 3, all the QA salts are obviously more resistant toward oxidation than $[C_2mmi][CF_3BF_3]$. This result suggests that the anodic stability of the former is determined by the involved anions, while that of the latter is essentially limited by the decomposition of the cation $[C_2mmi]^+$. This result is in keeping our previous conclusion that both the cathodic and anodic stability of 1,3-dlialkyimidazolium salts with electrochemically stable anions, such as $[R_FBF_3]^-$, $[BF_4]^-$, and $TFSI^-$, are limited by the cations but not by the anions.[43,45] However, as seen in Figure 9 and Table 3, the anodic stability of these anions is hardly distinguishable, since the E_{anodic} values for these QA salts are very close and show some dependence on the cations. Additionally, it should be noted that the previously reported improved anodic stability for the inorganic fluoroanion, $[BF_4]^-$, than for the organic fluoroanion, $TFSI^-$, was not observed in this study.[13,21,22] This may be attributed to the presence of relatively high amounts of water in our $[BF_4]^-$ salts (400–600 ppm), which reduces the anodic stability of the salts, as reported in the literature.[54]

Conclusion

A novel family of low-melting, hydrophobic ionic liquids containing small aliphatic quaternary ammoniums ($[R^1R^2R^3NR]^+$, wherein R^1, R^2, R^3 = CH_3 or C_2H_5, R = *n*-C_3H_7, *n*-C_4H_9, $CH_2CH_2OCH_3$) and perfluoroalkyltrifluoroborates ($[R_FBF_3]^-$, R_F = CF_3, C_2F_5, *n*-C_3F_7, *n*-C_4F_9) has been prepared and characterized. Most of them are liquids at room temperature and exhibit much lower viscosities (58–210 cP at 25 °C) than those with $[BF_4]^-$ (335–426 cP at 25 °C) owing to the relatively lower symmetry and better charge distribution of the $[R_FBF_3]^-$. Many of them exhibit plastic crystal behavior, which has a fundamental importance in all-solid-state electrolytes. More importantly, all these quaternary ammonium salts exhibit improved cathodic and anodic stability, hence larger electrochemical windows, than the corresponding 1,3-dialkyimidazolium salts. Because of these desirable properties, these new salts not only enrich the existing arsenal of quaternary ammonium ionic liquids, but may also serve as new media for some special organic and biocatalytic reactions and as electrolytes for high-energy devices and electrochemical processes in which the 1,3-dialkylimidazolium salts cannot operate.

Experimental Section

General: The following reagents and materials were used as received: dimethylethylamine, diethylmethylamine, triethylamine, 1-bromopropane, 1-bromobutane, 2-bromoethyl methyl ether (Tokyo Kasei); 30% aqueous trimethylamine; anhydrous diethyl ether, acetone, and tetrahydrofuran (H_2O < 30 ppm) (Wako Pure Chem.); bis(trifluoromethanesulfonyl)imide acid (Central Glass); 48% aqueous tetrafluoroboric acid (Aldrich); acidic cation-exchange and basic anion-exchange resins (Mitsubishi Chem., ion exchange capacity > 2.0 meq. mL^{-1}).

Potassium perfluoroalkyltrifluoroborates $K[R_FBF_3]$ (R_F = CF_3, C_2F_5, *n*-C_3F_7, and *n*-C_4F_9)[38,40] were prepared and purified according to the reported procedures.

^1H, ^{19}F, and ^{11}B NMR spectra were recorded on a JEOL JNM AL400 spectrometer operating at 399.65, 376.05, and 128.15 MHz, respectively. [D_4]Methanol was used the as solvent for the halide salts, and [D_6]acetone for the salts based on $[R_FBF_3]^-$, $[BF_4]^-$, and $TFSI^-$. Chemical shift values are reported relative to the TMS internal reference for ^1H, and external references CCl_3F in [D_6]acetone for ^{19}F (δ_F = 0.00) and $BF_3{\cdot}Et_2O$

in $CDCl_3$ for ^{11}B ($\delta_B = 0.00$). FAB-MS were measured on a JEOL JMS-HX110/110A spectrometer. Elemental analysis (C, H, and N) was performed at the Center for Organic Elemental Microanalysis of Kyoto University.

The water content in the liquid salts was determined by Karl-Fischer titration (Mitsubishi Chem., model CA-07).

The amounts of residual halide and potassium ions in the liquid salts were approximately estimated by a fluorescence X-ray spectrometer (JEOL, model JSX-3201) and revealed to be less than 30 ppm.

Phase transition analysis: The calorimetric measurements were performed with a differential scanning calorimeter (Perkin Elmer Pyris 1 DSC equipped with a liquid nitrogen cryostatic cooling) in the temperature range −150 °C to a predetermined temperature. An average sample weight of 5–10 mg was sealed in an aluminum pan, and then heated and cooled at a rate of 10 °C min^{-1} under a flow of helium. The glass transition temperature (T_g, onset of the heat capacity change), crystallization temperature (T_c, onset of the exothermic peak), solid–solid transition temperature ($T_{s\text{-}s}$, onset of the endothermic peak), and melting point (T_m, onset of the endothermic peak) were taken during heating in the second heating–cooling cycle.

Thermal gravimetric analysis (TGA): TGA was performed on a thermal analysis system (Seiko Instruments, TG/DTA 6200). An average sample weight of 5 mg was placed in a platinum pan and heated at 10 °C min^{-1} from ≈40 °C to 600 °C under a flow of nitrogen. The onset of decomposition was defined as the decomposition temperature (T_d).

Viscosity: The viscosity was measured with a spindle viscometer equipped with a thermostated water bath (Brookfield, model DV-III+, cone spindle: CP-52) at 25 °C. The measurements have a precision of ±2%.

Density: The density was the mean of three measurement values, which were approximately determined by measuring the weight of three separate samples (1.0 mL) at 25 °C. The relative standard uncertainty of the mean density was less than 5%.

Specific conductivity: The ionic conductivity (κ) of the neat liquid salts was measured by a conductivity meter (Radiometer Analytical, model CDM230) in a sealed conductivity cell at 25 °C.

Electrochemical stability: Linear sweep voltammetry (LSV) was performed with an automatic polarization system (ALS model 600) in an argon-filled glove box (O_2 and water < 5 ppm), with a 5 mL beaker-type three-electrode cell equipped with a glassy carbon electrode (surface area: 7.85×10^{-3} cm^{-2}), a Pt wire counterelectrode, and an I_3^-/I^- reference electrode consisting of Pt wire/0.015 mol dm^{-3} I_2 + 0.060 mol dm^{-3} [(n-C_3H_7)$_4$N]I in [C_2mim]TFSI ([C_2mim]$^+$ 1-ethyl-3-methylimidazolium). The potential was referred to ferrocene (Fc)/ferrocenium (Fc^+) redox couple in each salt. The data for each salt were collected in the first cathodic and anodic scan at 25 °C.

Procedure for quaternary ammonium bromides ([QA][Br]):

***N*,*N*-Diethyl-*N*-methyl-*N*-(*n*-propyl)ammonium bromide (N_{1223}Br)**: This compound was prepared in 0.30-mol scale in a 300 mL autoclave (Taiatsu Techno) by reaction of 1-bromopropane (37.0 g, 0.30 mol) with a small excess of ethyldimethylamine (27.0 g, 0.31 mol) in anhydrous acetone at 100 °C and ≈6 MPa for 12 h. The cooled red suspension was then poured into diethyl ether (150 mL). After filtration, the obtained solid was washed with diethyl ether (2×25 mL), and recrystallized twice from acetone to afford N_{1223}Br (50 g, yield 80%) as a white solid. T_m = 270 °C (decomp); ^{1}H NMR: δ = 1.02 (t, J = 7.2 Hz, 3H), 1.33 (t, J = 7.2 Hz, 2×3H), 1.78 (m, 2H), 3.00 (s, 3H), 3.23 (m, 2H), 3.38 ppm (q, J = 7.3 Hz, 2×2H).

***N*-(*n*-Butyl)-*N*,*N*-diethyl-*N*-methylammonium bromide (N_{1224}Br)**: The same procedure was followed as described for N_{1223}Br, except for the use of 1-bromobutane (41.1 g, 0.30 mol) instead of 1-bromopropane. Recrystallization twice from acetone/tetrahydrofuran (65:35) gave N_{1224}Br (54 g, yield 80%) as a white solid. T_m = 179 °C; T_d = 236 °C; ^{1}H NMR: δ = 1.02 (t, J = 7.4 Hz, 3H), 1.33 (t, J = 7.4 Hz, 2×3H), 1.40 (m, 2H), 1.71 (m, 2H), 2.99 (s, 3H), 3.25 (m, 2H), 3.36 ppm (m, 2×2H).

***N*,*N*,*N*-Trimethyl-*N*-(2-methoxyethyl)ammonium bromide ($N_{111.1O2}$Br)**: 2-Bromoethyl methyl ether (56.0 g, 0.40 mol) was added at room temperature to a solution of 30% aqueous trimethylamine (100 g solution, 0.51 mol amine). The reaction mixture was stirred at room temperature for three days. The excess amine and water was removed by evaporation at 70 °C under reduced pressure. The residual solid was washed with diethyl ether (2×25 mL). Recrystallization twice from acetone/2-butanol (75:25) gave $N_{111.1O2}$Br (50.5 g, yield 85%) as a white solid. T_m = 149 °C; T_d = 253 °C; ^{1}H NMR: δ = 3.21 (s, 3×3H), 3.40 (s, 3H), 3.62 (s, 2H), 3.82 ppm (s, 2H).

***N*-Ethyl-*N*,*N*-dimethyl-*N*-(2-methoxyethyl)ammonium bromide ($N_{112.1O2}$Br)**: The same procedure was followed as described for N_{1223}Br, except ethyldimethylamine (22.7 g, 0.31 mmol) and 2-bromoethyl methyl ether (41.7 g, 0.30 mol) were used. Recrystallization twice from acetone/2-butanol (85:15) gave $N_{112.1O2}$Br (50 g, yield 78%) as a white solid. T_m = 64 °C; T_d = 249 °C; ^{1}H NMR: δ = 1.37 (t, J = 7.2 Hz, 3H), 3.14 (s, 2×3H), 3.39 (s, 3H), 3.50 (q, 2×2H), 3.58 (t, J = 4.8 Hz, 2H), 3.81 ppm (s, 2H).

***N*,*N*-Diethyl-*N*-methyl-*N*-(2-methoxyethyl)ammonium bromide ($N_{122.1O2}$Br)**: The same procedure was followed as described for N_{1223}Br, except diethylmethylamine (27.0 g, 0.31 mol) and 2-bromoethyl methyl ether (41.7 g, 0.30 mol) were used. Recrystallization twice from acetone gave $N_{122.1O2}$Br (52 g, yield 76%) as a white solid. T_m = 85 °C; T_d = 236 °C; ^{1}H NMR: δ = 1.35 (t, J = 7.2 Hz, 2×3H), 3.08 (s, 3H), 3.39 (s, 3H), 3.48 (q, J = 7.1 Hz, 2×2H), 3.58 (t, J = 4.8 Hz, 2H), 3.82 ppm (s, 2H).

***N*,*N*,*N*-Triethyl-*N*-(2-methoxyethyl)ammonium bromide ($N_{222.1O2}$Br)**: The same procedure was followed as described for N_{1223}Br, except triethylamine (31.4 g, 0.31 mol) and 2-bromoethyl methyl ether (41.7 g, 0.30 mol) were used. Recrystallization twice from acetone/tetrahydrofuran (70:30) gave $N_{222.1O2}$Br (yield 80%) as a white solid. T_m = 106 °C; T_d = 224 °C; ^{1}H NMR: δ = 1.30 (t, J = 7.4 Hz, 3×3H), 3.38 (s, 3H), 3.43 (q, J = 7.2 Hz, 3×2H), 3.51 (t, J = 4.8 Hz, 2H), 3.77 ppm (s, 2H).

Procedure for aqueous solutions of perfluoroalkyltrifluoroborate acid ($H[R_FBF_3]$) and quaternary ammonium hydroxide ([QA][OH]):

Aqueous H[R_FBF$_3$]: Aqueous $H[R_FBF_3]$ was prepared by passing the corresponding $K[R_FBF_3]$ (R_F = CF_3, C_2F_5, n-C_3F_7, n-C_4F_9) through a column filled in acidic ion-exchange resin, as described in the literature.[38] The concentration of the aqueous $H[R_FBF_3]$, determined by acid–base titration, was ≈0.2 mol dm^{-3}. The resultant solution was collected in a PFA bottle, and stored in a refrigerator until required.

Aqueous [QA][OH]: The same procedure was followed for aqueous $H[R_FBF_3]$ as described above, except that the basic anion-exchange resin and the corresponding quaternary ammonium bromide ([QA][Br]) were used. The concentration of the aqueous [QA][OH] was ≈0.2 mol dm^{-3}. The solution was collected in a plastic bottle, and stored in a refrigerator until required.

Procedure for quaternary ammonium salts with perfluoroalkyltrifluoroborate ($[QA][R_FBF_3]$): The $[QA][R_FBF_3]$ salts were prepared in 30 mmol scale as follows: aqueous [QA][OH] was neutralized with equimolar aqueous $H[R_FBF_3]$ (R_F = CF_3, C_2F_5, n-C_3F_7, n-C_4F_9) in a PFA flask until the pH was ≈6–7. The mixture was concentrated to ≈15 mL at 40 °C by evaporation under reduced pressure. The liquid salt precipitated in the bottom was separated directly, washed with deionized water (5 mL) and toluene (10 mL) in turn, and dried at 70 °C for 24 h under vacuum (0.03 Torr) to afford a colorless or pale yellow liquid (water content < 50 ppm). The solid salt was collected by filtration, dried under vacuum, and recrystallized from 2-butanol to afford a white product.

***N*,*N*-Diethyl-*N*-methyl-*N*-(*n*-propyl)ammonium trifluoromethyltrifluoroborate ($N_{1223}[CF_3BF_3]$)**: Yield: 75%, white solid; ^{1}H NMR: δ = 1.01 (t, J = 7.4 Hz, 3H), 1.42 (t, J = 7.4 Hz, 2×3H), 1.87 (m, 2H). 3.13 (s, 3H), 3.38 (m, 2H), 3.53 ppm (q, J = 7.3 Hz, 2×2H); ^{19}F NMR: δ = −74.6 (q, ^2J(B,F) = 32.6 Hz, 3F; CF_3), −155.5 ppm (q, ^1J(B,F) = 39.6 Hz, 3F; BF_3); ^{11}B NMR: δ = −0.49 ppm (qq, ^1J(B,F) = 39.0 Hz, ^2J(B,F) = 32.3 Hz); FAB-MS: m/z (%): 130 (100) $[N_{1223}]^+$, 137 (100) $[CF_3BF_3]^-$; elemental analysis calcd (%) for $C_9H_{20}BF_6N$ (267.06): C 40.5, H 7.6, N 5.2; found: C 40.3, H 7.4, N 5.3.

***N*-(*n*-Butyl)-*N*,*N*-diethyl-*N*-methylammonium trifluoromethyltrifluoroborate ($N_{1224}[CF_3BF_3]$)**: Yield: 77%, colorless liquid; ^{1}H NMR: δ = 0.99 (t, J = 7.2 Hz, 3H), 1.40 (t, J = 7.2 Hz, 2×3H), 1.44 (t, J = 7.4 Hz, 2H),

1.81 (m, 2H), 3.12 (s, 3H), 3.38 (m, 2H), 3.50 ppm (q, J = 7.3 Hz, 2×2H); ^{19}F NMR: δ = −74.6 (q, ^{2}J(B,F) = 31.6 Hz, 3F; CF_3), −155.5 ppm (q, ^{1}J(B,F) = 38.6 Hz, 3F; BF_3); ^{11}B NMR: δ = −0.48 ppm (qq, ^{1}J(B,F) = 39.9 Hz, ^{2}J(B,F) = 32.3 Hz); FAB-MS: m/z (%): 144 (100) $[N_{1224}]^+$, 137 (100) $[CF_3BF_3]^-$; elemental analysis calcd (%) for $C_{10}H_{22}BF_6N$ (281.09): C 42.7, H 7.9, N 5.0; found: C 42.7, H 7.6, N 5.0.

N,N,N-Trimethyl-N-(2-methoxyethyl)ammonium trifluoromethyltrifluoroborate ($N_{111.1O2}[CF_3BF_3]$): Yield: 80%, white solid; ^{1}H NMR: δ = 3.37 (s, 3×3H), 3.40 (s, 3H), 3.78 (s, 2H), 3.95 ppm (s, 2H); ^{19}F NMR: δ = −74.6 (q, ^{2}J(B,F) = 31.6 Hz, 3F; CF_3), −155.5 ppm (q, ^{1}J(B,F) = 38.6 Hz, 3F; BF_3); ^{11}B NMR: δ = −0.52 ppm (qq, ^{1}J(B,F) = 39.9 Hz, ^{2}J(B,F) = 32.3 Hz); FAB-MS: m/z (%): 118 (100) $[N_{111.1O2}]^+$, 137 (100) $[CF_3BF_3]^-$; elemental analysis calcd (%) for $C_7H_{16}BF_6NO$ (255.01): C 33.0, H 6.3, N 5.5; found: C 32.7, H 6.3, N 5.6.

***N*-ethyl-N,N-Dimethyl-N-(2-methoxyethyl)ammonium trifluoromethyltrifluoroborate ($N_{112.1O2}$ $[CF_3BF_3]$)**: Yield: 66%, pale yellow liquid; ^{1}H NMR: δ = 1.44 (t, J = 7.2 Hz, 3H), 3.26 (s, 2×3H), 3.39 (s, 3H), 3.62 (q, J = 7.2 Hz, 2H), 3.69 (t, J = 4.8 Hz, 2H), 3.91 ppm (s, 2H); ^{19}F NMR: δ = −74.7 (q, ^{2}J(B,F) = 31.6 Hz, 3F; CF_3), −155.0 ppm (q, ^{1}J(B,F) = 39.6 Hz, 3F; BF_3); ^{11}B NMR: δ = −0.53 ppm (qq, ^{1}J(B,F) = 39.0 Hz, ^{2}J(B,F) = 32.3 Hz); FAB-MS: m/z (%): 132 (100) $[N_{112.1O2}]^+$, 137 (100) $[CF_3BF_3]^-$; elemental analysis calcd (%) for $C_8H_{18}BF_6NO$ (269.03): C 35.7, H 6.7, N 5.2; found: C 35.3, H 6.7, N 5.3.

N,N-Diethyl-N-methyl-N-(2-methoxyethyl)ammonium trifluoromethyltrifluoroborate ($N_{122.1O2}[CF_3BF_3]$): Yield: 70%, colorless liquid; ^{1}H NMR: δ = 1.41 (t, J = 7.2 Hz, 2×3H), 3.20 (s, 3H), 3.38 (s, 3H), 3.59 (q, J = 7.3 Hz, 2×2H), 3.68 (t, J = 4.8 Hz, 2H), 3.90 (s, 2H); ^{19}F NMR: δ = −74.7 (q, ^{2}J(B,F) = 32.6 Hz, 3F; CF_3), −155.3 ppm (q, ^{1}J(B,F) = 38.7 Hz, 3F; BF_3); ^{11}B NMR: δ = −0.49 ppm (qq, ^{1}J(B,F) = 38.9 Hz, ^{2}J(B,F) = 32.3 Hz); FAB-MS: m/z (%): 146 (100) $[N_{122.1O2}]^+$, 137 (100) $[CF_3BF_3]^-$; elemental analysis calcd (%) for $C_9H_{20}BF_6NO$ (283.06): C 38.2, H 7.1, N 5.0; found: C 38.0, H 7.1, N 5.1.

N,N,N-Triethyl-N-(2-methoxyethyl)ammonium trifluoromethyltrifluoroborate ($N_{222.1O2}[CF_3BF_3]$): Yield: 85%, white solid; ^{1}H NMR: δ = 1.38 (t, J = 7.2 Hz, 3×3H), 3.38 (s, 3H), 3.54 (q, J = 7.2 Hz, 3×2H), 3.63 (t, J = 4.8 Hz, 2H), 3.87 ppm (s, 2H); ^{19}F NMR: δ = −74.6 (q, ^{2}J(B,F) = 31.5 Hz, 3F; CF_3), −155.4 ppm (q, ^{1}J(B,F) = 39.6 Hz, 3F; BF_3); ^{11}B NMR: δ = −0.48 ppm (qq, ^{1}J(B,F) = 39.0 Hz, ^{2}J(B,F) = 32.3 Hz); FAB-MS: m/z (%): 160 (100) $[N_{222.1O2}]^+$, 137 (100) $[CF_3BF_3]^-$; elemental analysis calcd (%) for $C_{10}H_{22}BF_6NO$ (297.09): C 40.4, H 7.5, N 4.7; found: C 40.5, H 7.5, N 4.7.

N,N-Diethyl-N-methyl-N-(n-propyl)ammonium pentafluoroethyltrifluoroborate ($N_{1223}[C_2F_5BF_3]$): Yield: 90%, white solid; ^{1}H NMR: δ = 1.02 (t, J = 7.4 Hz, 3H), 1.42 (t, J = 7.2 Hz, 2×3H), 1.86 (m, 2H), 3.15 (s, 3H), 3.38 (t, 2H), 3.53 ppm (q, J = 7.2 Hz, 2×2H); ^{19}F NMR: δ = −83.1 (s, 3F; CF_3), −135.9 (q, ^{2}J(B,F) = 19.3 Hz, 2F; CF_2), −153.1 ppm (q, ^{1}J(B,F) = 41.0 Hz, 3F; BF_3); ^{11}B NMR: δ = 0.21 ppm (qt, ^{1}J(B,F) = 40.6 Hz, ^{2}J(B,F) = 19.86 Hz); FAB-MS: m/z (%): 130 (100) $[N_{1223}]^+$, 187 (100) $[C_2F_5BF_3]^-$; elemental analysis calcd (%) for $C_{10}H_{20}BF_8N$ (317.07): C 37.9, H 6.4, N 4.4; Found: C 37.8, H 6.1, N 4.5.

***N*-(n-Butyl)-N,N-diethyl-N-methylammonium pentafluoroethyltrifluoroborate ($N_{1224}[C_2F_5BF_3]$)**: Yield: 88%, colorless liquid; ^{1}H NMR: δ = 0.99 (t, J = 7.2 Hz, 3H), 1.40 (t, J = 7.4 Hz, 2×3H), 1.46 (t, J = 7.2 Hz, 2H), 1.81 (m, 2H), 3.12 (s, 3H), 3.38 (m, 2H), 3.50 ppm (q, J = 7.2 Hz, 2×2H); ^{19}F NMR: δ = −83.0 (s, 3F; CF_3), −135.8 (q, ^{2}J(B,F) = 19.9 Hz, 2F; CF_2), −152.8 ppm (q, ^{1}J(B,F) = 39.6 Hz, 3F; BF_3); ^{11}B NMR: δ = 0.21 ppm (qt, ^{1}J(B,F) = 40.6 Hz, ^{2}J(B,F) = 19.9 Hz); FAB-MS: m/z (%): 144 (100) $[N_{1224}]^+$, 187 (100) $[C_2F_5BF_3]^-$; elemental analysis calcd (%) for $C_{11}H_{22}BF_8N$ (331.1): C 39.9, H, 6.7, N 4.2; found: C 39.7, H, 6.4, N 4.2.

N,N,N-Trimethyl-N-(2-methoxyethyl)ammonium pentafluoroethyltrifluoroborate ($N_{111.1O2}[C_2F_5BF_3]$): Yield: 86%, white solid; ^{1}H NMR: δ = 3.37 (s, 3×3H), 3.40 (s, 3H), 3.76 (s, 2H), 3.94 ppm (s, 2H); ^{19}F NMR: δ = −83.0 (s, 3F; CF_3), −135.8 (q, ^{2}J(B,F) = 19.3 Hz, 2F; CF_2), −153.0 ppm (q, ^{1}J(B,F) = 39.6 Hz, 3F; BF_3); ^{11}B NMR: δ = 0.22 ppm (qt, ^{1}J(B,F) = 40.9 Hz, ^{2}J(B,F) = 19.1 Hz); FAB-MS: m/z (%): 118 (100) $[N_{111.1O2}]^+$, 187 (100) $[C_2F_5BF_3]^-$; elemental analysis calcd (%) for $C_8H_{16}BF_8NO$ (305.02): C 31.5, H 5.3, N 4.6; found: C 31.2, H 5.2, N 4.6.

***N*-Ethyl-N,N-dimethyl-N-(2-methoxyethyl)ammonium pentafluoroethyltrifluoroborate ($N_{112.1O2}$ $[C_2F_5BF_3]$)**: Yield: 88%, pale yellow liquid; ^{1}H NMR: δ = 1.45 (t, J = 7.2 Hz, 3H), 3.28 (s, 2×3H), 3.39 (s, 3H), 3.64 (q, J = 7.2 Hz, 2H), 3.71 (t, J = 4.8 Hz, 2H), 3.92 ppm (s, 2H); ^{19}F NMR: δ = −83.0 (s, 3F; CF_3), −135.8 (q, ^{2}J(B,F) = 19.3 Hz, 2F; CF_2), −152.7 ppm (q, ^{1}J(B,F) = 40.7 Hz, 3F; BF_3); ^{11}B NMR: δ = 0.21 ppm (qt, ^{1}J(B,F) = 40.9 Hz, ^{2}J(B,F) = 19.1 Hz); FAB-MS: m/z (%): 132 (100) $[N_{112.1O2}]^+$, 187 (100) $[C_2F_5BF_3]^-$; elemental analysis calcd (%) for $C_9H_{18}BF_8NO$ (319.04): C 33.9, H 5.7, N 4.4; found: C 33.7, H 5.6, N 4.3.

N,N-Diethyl-N-methyl-N-(2-methoxyethyl)ammonium pentafluoroethyltrifluoroborate ($N_{122.1O2}[n\text{-}C_2F_5BF_3]$): Yield: 90%, colorless liquid; ^{1}H NMR: δ = 1.41 (t, J = 7.2 Hz, 2×3H), 3.19 (s, 3H), 3.39 (s, 3H), 3.59 (q, J = 7.2 Hz, 2×2H), 3.67 (t, J = 4.8 Hz, 2H), 3.91 ppm (s, 2H); ^{19}F NMR: δ = −83.0 (s, 3F; CF_3), −135.8 (q, ^{2}J(B,F) = 20.3 Hz, 2F; CF_2), −152.8 ppm (q, ^{1}J(B,F) = 40.7 Hz, 3F; BF_3); ^{11}B NMR: δ = 0.15 ppm (qt, ^{1}J(B,F) = 40.8 Hz, ^{2}J(B,F) = 19.1 Hz); FAB-MS: m/z (%): 146 (100) $[N_{122.1O2}]^+$, 187 (100) $[C_2F_5BF_3]^-$; elemental analysis calcd (%) for $C_{10}H_{20}BF_8NO$ (333.07): C 36.1, H 6.1, N 4.2; found: C 35.8, H 5.9, N 4.1.

N,N,N-Triethyl-N-(2-methoxyethyl)ammonium pentafluoroethyltrifluoroborate ($N_{222.1O2}[C_2F_5BF_3]$): Yield: 90%, colorless liquid; ^{1}H NMR: δ = 1.37 (t, J = 7.2 Hz, 3×3H), 3.38 (s, 3H), 3.56 (q, J = 7.2 Hz, 3×2H), 3.63 (t, J = 4.8 Hz, 2H), 3.87 ppm (s, 2H); ^{19}F NMR: δ = −83.0 (s, 3F; CF_3), −135.8 (q, ^{2}J(B,F) = 19.4 Hz, 2F; CF_2), −153.0 ppm (q, ^{1}J(B,F) = 39.7 Hz, 3F; BF_3); ^{11}B NMR: δ = 0.19 ppm (qt, ^{1}J(B,F) = 40.9 Hz, ^{2}J(B,F) = 19.1 Hz); FAB-MS: m/z (%): 160 (100) $[N_{222.1O2}]^+$, 187 (100) $[C_2F_5BF_3]^-$; elemental analysis calcd (%) for $C_{11}H_{22}BF_8NO$ (347.1): C 38.1, H 6.4, N 4.0; found: C 38.1, H 6.4, N 4.0.

N,N-Diethyl-N-methyl-N-(n-propyl)ammonium (heptafluoro-n-propyl)trifluoroborate ($N_{1223}[n\text{-}C_3F_7BF_3]$): Yield: 88%, white solid; ^{1}H NMR: δ = 1.01 (t, J = 7.4 Hz, 3H), 1.41 (t, J = 7.2 Hz, 2×3H), 1.88 (m, 2H), 3.15 (s, 3H), 3.38 (m, 2H), 3.53 (q, J = 7.2 Hz, 2×2H); ^{19}F NMR: δ = −80.5 (s, 3F; CF_3), −127.6 (s, 2F; $BCCF_2$-), −133.8 (s, 2F; CF_2B), −152.4 ppm (q, ^{1}J(B,F) = 40.7 Hz, 3F; BF_3); ^{11}B NMR: δ = 0.25 ppm (qt, ^{1}J(B,F) = 40.3 Hz, ^{2}J(B,F) = 19.9 Hz); FAB-MS: m/z (%): 130 (100) $[N_{1223}]^+$, 237 (100) $[C_3F_7BF_3]^-$; elemental analysis calcd (%) for $C_{11}H_{20}BF_{10}N$ (367.08): C 36.0, H 5.5, N 3.8; found: C 35.8, H 5.2, N 3.9.

***N*-(n-Butyl)-N,N-diethyl-N-methylammonium (heptafluoro-N-propyl)trifluoroborate ($N_{1224}[n\text{-}C_3F_7BF_3]$)**: Yield: 88%, white solid; ^{1}H NMR: δ = 0.99 (t, J = 7.2 Hz, 3H), 1.40 (t, J = 7.4 Hz, 2×3H), 1.46 (t, J = 7.4 Hz, 2H), 1.82 (m, 2H), 3.12 (s, 3H), 3.38 (m, 2H), 3.50 ppm (q, J = 7.2 Hz, 2×2H); ^{19}F NMR: δ = −80.4 (s, 3F; CF_3), −127.5 (s, 2F; $BCCF_2$-), −133.7 (s, 2F; CF_2B), −152.3 ppm (q, ^{1}J(B,F) = 40.0 Hz, 3F; BF_3); ^{11}B NMR: δ = 0.25 ppm (qt, ^{1}J(B,F) = 40.6 Hz, ^{2}J(B,F) = 19.1 Hz); FAB-MS: m/z (%): 144 (100) $[N_{1224}]^+$, 237 (100) $[C_3F_7BF_3]^-$; elemental analysis calcd (%) for $C_{12}H_{22}BF_{10}N$ (381.11): C 37.8, H 5.8, N 3.7; found: C 37.7, H 5.6, N 3.9.

N,N,N-Trimethyl-N-(2-methoxyethyl)ammonium (heptafluoro-n-propyl)trifluoroborate ($N_{111.1O2}[n\text{-}C_3F_7BF_3]$): Yield: 88%, colorless liquid; ^{1}H NMR: δ = 3.36 (s, 3×3H), 3.40 (s, 3H), 3.77 (s, 2H), 3.95 ppm (s, 2H); ^{19}F NMR: δ = −80.5 (s, 3F; CF_3), −127.6 (s, 2F; $BCCF_2$-), −133.7 (s, 2F; CF_2B), −152.3 ppm (q, ^{1}J(B,F) = 39.6 Hz, 3F; BF_3); ^{11}B NMR: δ = 0.25 ppm (qt, ^{1}J(B,F) = 40.6 Hz, ^{2}J(B,F) = 19.0 Hz); FAB-MS: m/z (%): 118 (100) $[N_{111.1O2}]^+$, 237 (100) $[C_3F_7BF_3]^-$; elemental analysis calcd (%) for $C_9H_{16}BF_{10}NO$ (355.03): C 30.5, H 4.5, N 4.0; found: C 30.4, H 4.5, N 4.2.

***N*-ethyl-N,N-dimethyl-N-(2-methoxyethyl)ammonium (heptafluoro-n-propyl)trifluoroborate ($N_{112.1O2}[n\text{-}C_3F_7BF_3]$)**: Yield: 90%, pale yellow liquid; ^{1}H NMR: δ = 1.45 (t, J = 7.1 Hz, 3H), 3.28 (s, 2×3H), 3.39 (s, 3H), 3.65 (q, J = 7.1 Hz, 2H), 3.72 (t, J = 4.6 Hz, 2H), 3.93 ppm (s, 2H); ^{19}F NMR: δ = −80.5 (s, 3F; CF_3), −127.5 (s, 2F; $BCCF_2$-), −133.6 (s, 2F; CF_2B), −152.3 ppm (q, ^{1}J(B,F) = 40.6 Hz, 3F; BF_3); ^{11}B NMR: δ = 0.26 ppm (qt, ^{1}J(B,F) = 40.6 Hz, ^{2}J(B,F) = 19.0 Hz); FAB-MS: m/z (%): 132 (100) $[N_{112.1O2}]^+$, 237 (100) $[C_3F_7BF_3]^-$; elemental analysis calcd (%) for $C_{10}H_{18}BF_{10}NO$ (369.05): C 32.5, H 4.9, N 3.8; found: C 32.3, H 4.7, N 4.1.

***N,N*-Diethyl-*N*-methyl-*N*-(2-methoxyethyl)ammonium (heptafluoro-*n*-propyl)trifluoroborate ($N_{122.1O2}[n\text{-}C_3F_7BF_3]$)**: Yield: 90%, colorless liquid; ^{1}H NMR: δ = 1.41 (t, J = 7.3 Hz, 2×3H), 3.20 (s, 3H), 3.38 (s, 3H), 3.59 (q, J = 7.2 Hz, 2×2H), 3.67 (t, J = 4.8 Hz, 2H), 3.91 ppm (s, 2H); ^{19}F NMR: δ = −80.3 (s, 3F; CF_3), −127.5 (s, 2F; $BCCF_2$-), −133.7 (s, 2F; CF_2B), −152.3 ppm (q, ^1J(B,F) = 38.7 Hz, 3F; BF_3); ^{11}B NMR: δ = 0.25 ppm (qt, ^1J(B,F) = 40.6 Hz, ^2J(B,F) = 19.0 Hz); FAB-MS: m/z (%): 146 (100) $[N_{122.1O2}]^+$, 237 (100) $[C_3F_7BF_3]^-$; elemental analysis calcd (%) for $C_{11}H_{20}BF_{10}NO$ (383.08): C 34.5, H 5.3, N 3.7; found: C 34.8, H 5.4, N 3.6.

***N,N,N*-Triethyl-*N*-(2-methoxyethyl)ammonium (heptafluoro-*n*-propyl)trifluoroborate ($N_{222.1O2}[n\text{-}C_3F_7BF_3]$)**: Yield: 90%, colorless liquid; ^{1}H NMR: δ = 1.38 (t, J = 7.2 Hz, 3×3H), 3.38 (s, 3H), 3.56 (q, J = 7.3 Hz, 3×2H), 3.64 (t, J = 4.6 Hz, 2H), 3.88 ppm (s, 2H); ^{19}F NMR: δ = −80.4 (s, 3F; CF_3), −127.5 (s, 2F; $BCCF_2$-), −133.7 (s, 2F; CF_2B), −152.5 ppm (q, ^1J(B,F) = 40.7 Hz, 3F; BF_3); ^{11}B NMR: δ = 0.24 ppm (qt, ^1J(B,F) = 40.3 Hz, ^2J(B,F) = 19.1 Hz); FAB-MS: m/z (%): 160 (100) $[N_{222.1O2}]^+$, 237 (100) $[C_3F_7BF_3]^-$; elemental analysis calcd (%) for $C_{12}H_{22}BF_{10}NO$ (397.11): C 36.3, H 5.6, N 3.5; found: C 36.3, H 5.5, N 3.6.

***N,N*-Diethyl-*N*-methyl-*N*-(*n*-propyl)ammonium (nonafluoro-*n*-butyl)trifluoroborate ($N_{1223}[n\text{-}C_4F_9BF_3]$)**: Yield: 90%, white solid; ^{1}H NMR: δ = 1.01 (t, J = 7.4 Hz, 3H), 1.42 (t, J = 7.2 Hz, 2×3H), 1.86 (m, 2H). 3.15 (s, 3H), 3.38 (m, 2H), 3.53 ppm (q, J = 7.2 Hz, 2×2H); ^{19}F NMR: δ = −80.9 (s, 3F; CF_3), −123.9 (s, 2F; $BCCCF_2$-), −125.9 (s, 2F; $BCCF_2$-), −133.1 (s, 2F; CF_2B), −152.2 ppm (q, ^1J(B,F) = 40.6 Hz, 3F; BF_3); ^{11}B NMR: δ = 0.25 ppm (qt, ^1J(B,F) = 40.3 Hz, ^2J(B,F) = 19.0 Hz); FAB-MS: m/z (%): 130 (100) $[N_{1223}]^+$, 287 (100) $[C_4F_9BF_3]^-$; elemental analysis calcd (%) for $C_{12}H_{20}BF_{12}N$ (417.09): C 34.6, H 4.8, N 3.4; found: C 34.3, H 4.7, N 3.4.

***N*-(*n*-Butyl)-*N,N*-diethyl-*N*-methylammonium (nonafluoro-*n*-butyl)trifluoroborate ($N_{1224}[n\text{-}C_4F_9BF_3]$)**: Yield: 92%, white solid; ^{1}H NMR: δ = 0.99 (t, J = 7.4 Hz, 3H), 1.40 (t, J = 7.4 Hz, 2×3H), 1.46 (t, J = 7.2 Hz, 2H), 1.82 (m, 2H), 3.14 (s, 3H), 3.41 (m, 2H), 3.52 ppm (q, J = 7.2 Hz, 2×2H); ^{19}F NMR: δ = −80.9 (s, 3F; CF_3), −123.8 (s, 2F; $BCCCF_2$-), −125.8 (s, 2F; $BCCF_2$-), −133.0 (s, 2F; CF_2B), −152.2 ppm (q, ^1J(B,F) = 38.6 Hz, 3F; BF_3); ^{11}B NMR: δ = 0.25 ppm (qt, ^1J(B,F) = 40.3 Hz, ^2J(B,F) = 20.0 Hz); FAB-MS: m/z (%): 144 (100) $[N_{1224}]^+$, 287 (100) $[C_4F_9BF_3]^-$; elemental analysis calcd (%) for $C_{13}H_{22}BF_{12}N$ (431.12): C 36.2, H 5.1, N 3.3; found: C 36.0, H 5.0, N 3.5.

***N,N,N*-Trimethyl-*N*-(2-methoxyethyl)ammonium (nonafluoro-*n*-butyl)trifluoroborate ($N_{111.1O2}[n\text{-}C_4F_9BF_3]$)**: Yield: 90%, white solid; ^{1}H NMR: δ = 3.37 (s, 3×3H), 3.40 (s, 3H), 3.80 (s, 2H), 3.96 ppm (s, 2H); ^{19}F NMR: δ = −80.9 (s, 3F; CF_3), −123.8 (s, 2F; $BCCCF_2$-), −125.8 (s, 2F; $BCCF_2$-), −133.0 (s, 2F; CF_2B), −152.2 ppm (q, ^1J(B,F) = 38.6 Hz, 3F; BF_3); ^{11}B NMR: δ = 0.25 ppm (qt, ^1J(B,F) = 40.3 Hz, ^2J(B,F) = 19.0 Hz); FAB-MS: m/z (%): 118 (100) $[N_{111.1O2}]^+$, 287 (100) $[C_4F_9BF_3]^-$; elemental analysis calcd (%) for $C_{10}H_{16}BF_{12}NO$ (405.04): C 29.7, H 4.0, N 3.5; found: C 29.4, H 3.9, N 3.7.

***N*-Ethyl-*N,N*-dimethyl-*N*-(2-methoxyethyl)ammonium (nonafluoro-*n*-butyl)trifluoroborate ($N_{112.1O2}[n\text{-}C_4F_9BF_3]$)**: Yield: 90%, pale yellow liquid; ^{1}H NMR: δ = 1.46 (t, J = 7.4 Hz, 3H), 3.29 (s, 2×3H), 3.39 (s, 3H), 3.65 (q, J = 7.3 Hz, 2H), 3.72 (t, J = 4.8 Hz, 2H), 3.93 ppm (s, 2H); ^{19}F NMR: δ = −80.9 (s, 3F; CF_3), −123.8 (s, 2F; $BCCCF_2$-), −125.8 (s, 2F; $BCCF_2$-), −133.0 (s, 2F; CF_2B), −152.5 ppm (q, ^1J(B,F) = 38.1 Hz, 3F; BF_3); ^{11}B NMR: δ = 0.25 ppm (qt, ^1J(B,F) = 40.3 Hz, ^2J(B,F) = 19.9 Hz); FAB-MS: m/z (%): 132 (100) $[N_{112.1O2}]^+$, 287 (100) $[C_4F_9BF_3]^-$; elemental analysis calcd (%) for $C_{11}H_{18}BF_{12}NO$ (419.06): C 31.5, H 4.3, N 3.3; found: C 31.2, H 4.3, N 3.7.

***N,N*-Diethyl-*N*-methyl-*N*-(2-methoxyethyl)ammonium (nonafluoro-*n*-butyl)trifluoroborate ($N_{122.1O2}[n\text{-}C_4F_9BF_3]$)**: Yield: 91%, colorless liquid; ^{1}H NMR: δ = 1.41 (m, 2×3H), 3.21 (m, 3H), 3.38 (m, 3H), 3.60 (q, J = 7.2 Hz, 2×2H), 3.67 (t, J = 4.8 Hz, 2H), 3.91 ppm (s, 2H); ^{19}F NMR: δ = −80.9 (s, 3F; CF_3), −123.8 (s, 2F; $BCCCF_2$-), −125.8 (s, 2F; $BCCF_2$-), −133.1 (s, 2F; CF_2B), −152.3 ppm (q, ^1J(B,F) = 38.7 Hz, 3F; BF_3); ^{11}B NMR: δ = 0.23 ppm (qt, ^1J(B,F) = 40.3 Hz, ^2J(B,F) = 19.0 Hz); FAB-MS: m/z (%): 146 (100) $[N_{122.1O2}]^+$, 287 (100) $[C_4F_9BF_3]^-$; elemental analysis calcd (%) for $C_{12}H_{20}BF_{12}NO$ (433.09): C 33.3, H 4.7, N 3.2; found: C 33.1; H 4.6, N 3.1.

***N,N,N*-Triethyl-*N*-(2-methoxyethyl)ammonium (nonafluoro-*n*-butyl)trifluoroborate ($N_{222.1O2}[n\text{-}C_4F_9BF_3]$)**: Yield: 92%, colorless liquid; ^{1}H NMR: δ = 1.36 (t, J = 7.2 Hz, 3×3H), 3.36 (s, 3H), 3.54 (q, J = 7.2 Hz, 3×2H), 3.63 (t, J = 4.6 Hz, 2H), 3.86 ppm (s, 2H); ^{19}F NMR: δ = −80.9 (s, 3F; CF_3), −123.8 (s, 2F; $BCCCF_2$-), −125.8 (s, 2F; $BCCF_2$-), −133.0 (s, 2F; CF_2B), −152.3 ppm (q, ^1J(B,F) = 40.6 Hz, 3F; BF_3); ^{11}B NMR: δ = 0.23 ppm (qt, ^1J(B,F) = 40.6 Hz, ^2J(B,F) = 19.1 Hz); FAB-MS: m/z (%): 160 (100) $[N_{222.1O2}]^+$, 287 (100) $[C_4F_9BF_3]^-$; elemental analysis calcd (%) for $C_{13}H_{22}BF_{12}NO$ (447.12): C 34.9, H 5.0, N 3.1; found: C 34.9, H 4.8, N 3.2.

Procedure for quaternary ammonium salts with tetrafluoroborate ([QA][BF_4]): The [QA][BF_4] salts were prepared in a 50 mmol scale as follows: aqueous [QA][OH] was neutralized with equimolar aqueous H[BF_4] in a PFA flask until the pH was ≈6–7. The solution was evaporated at 30–40 °C under reduced pressure to give a viscous liquid or solid. If a viscous liquid was obtained, it was dried at 40 °C for 48 h at room temperature under vacuum (0.03 Torr), then dissolved in anhydrous acetone (60 mL), and filtered through a PTFE membrane filter (0.2 μm). The collected solution was evaporated and dried at 80 °C for 48 h under vacuum (0.03 Torr), yielding a pale yellow or colorless liquid (water content: ≈400–600 ppm). If a solid product was obtained, it was recrystallization from 2-butanol/methanol to give a white solid.

***N,N*-Diethyl-*N*-methyl-*N*-(*n*-propyl)ammonium tetrafluoroborate ($N_{1223}[BF_4]$)**: Yield: 88%, white solid; ^{1}H NMR: δ = 1.01 (t, J = 7.2 Hz, 3H), 1.39 (t, J = 7.2 Hz, 2×3H), 1.86 (m, 2H), 3.13 (s, 3H), 3.37 (m, 2H), 3.53 ppm (q, J = 7.3 Hz, 2×2H); ^{19}F NMR: δ = −150.0 ppm (s); ^{11}B NMR: δ = −0.23 ppm (s); FAB-MS: m/z (%): 130 (100) $[N_{1223}]^+$, 87 (100) $[BF_4]^-$; elemental analysis calcd (%) for $C_8H_{20}BF_4N$ (217.06): C 44.3, H 9.3, N 6.5; found: C 43.8, H 9.1, N 6.4.

***N*-(*n*-Butyl)-*N,N*-diethyl-*N*-methylammonium tetrafluoroborate ($N_{1224}[BF_4]$)**: Yield: 91%, white solid; ^{1}H NMR: δ = 0.99 (t, J = 7.4 Hz, 3H), 1.41 (t, J = 7.2 Hz, 2×3H), 1.47 (t, J = 7.4 Hz, 2H), 1.82 (m, 2H), 3.15 (s, 3H), 3.41 (m, 2H), 3.53 ppm (q, J = 7.3 Hz, 2×2H); ^{19}F NMR: δ = −150.2 ppm (s); ^{11}B NMR: δ = 0.21 ppm (s); FAB-MS: m/z (%): 144 (100) $[N_{1223}]^+$, 87 (100) $[BF_4]^-$; elemental analysis calcd (%) for $C_9H_{22}BF_4N$ (231.09): C 46.8, H 9.6, N 6.1; found: C 46.5, H 9.5, N 6.0.

***N,N,N*-Trimethyl-*N*-(2-methoxyethyl)ammonium tetrafluoroborate ($N_{111.1O2}[BF_4]$)**: Yield: 89%, white solid; ^{1}H NMR: δ = 3.34 (s, 3×3H), 3.40 (s, 3H), 3.74 (s, 2H), 3.92 ppm (s, 2H); ^{19}F NMR: δ = −149.3 ppm (s); ^{11}B NMR: δ = −0.23 ppm (s); FAB-MS: m/z (%): 118 (100) $[N_{111.1O2}]^+$, 87 (100) $[BF_4]^-$; elemental analysis calcd (%) for $C_6H_{16}BF_4NO$ (205.01): C 35.2, H 7.9, N 6.8; found: C 35.2, H 7.9, N 6.8.

***N*-Ethyl-*N,N*-dimethyl-*N*-(2-methoxyethyl)ammonium tetrafluoroborate ($N_{112.1O2}[BF_4]$)**: Yield: 90%, pale yellow liquid; ^{1}H NMR: δ = 1.42 (t, J = 7.2 Hz, 3H), 3.24 (s, 2×3H), 3.39 (s, 3H), 3.62 (q, J = 7.2 Hz, 2H), 3.69 (t, J = 4.8 Hz, 2H), 3.90 ppm (s, 2H); ^{19}F NMR: δ = −149.5 ppm (s); ^{11}B NMR: δ = −0.25 ppm (s); FAB-MS: m/z (%): 132 (100) $[N_{112.1O2}]^+$, 87 (100) $[BF_4]^-$; elemental analysis calcd (%) for $C_7H_{18}BF_4NO$ (219.03): C 38.4, H 8.3, N 6.4; found: C 38.4, H 8.8, N 6.4.

***N,N*-Diethyl-*N*-methyl-*N*-(2-methoxyethyl)ammonium tetrafluoroborate ($N_{122.1O2}[BF_4]$)**: Yield: 90%, colorless liquid; ^{1}H NMR: δ = 1.39 (t, J = 7.2 Hz, 2×3H), 3.15 (s, 3H), 3.38 (s, 3H), 3.57 (q, J = 7.3 Hz, 2×2H), 3.63 (t, J = 4.8 Hz, 2H), 3.88 ppm (s, 2H); ^{19}F NMR: δ = −149.8 ppm (s); ^{11}B NMR: δ = −0.25 ppm (s); FAB-MS: m/z (%): 146 (100) $[N_{122.1O2}]^+$, 87 (100) $[BF_4]^-$; elemental analysis calcd (%) for $C_8H_{20}BF_4NO$ (233.06): C 41.2, H 8.7, N 6.0; found: C 40.9, H 9.2, N 6.0.

***N,N,N*-Triethyl-*N*-(2-methoxyethyl)ammonium tetrafluoroborate ($N_{222.1O2}[BF_4]$)**: Yield: 92%, white solid; ^{1}H NMR: δ = 1.38 (t, J = 7.2 Hz, 3×3H), 3.38 (s, 3H), 3.54 (q, J = 7.2 Hz, 3×2H), 3.64 (t, J = 4.8 Hz, 2H), 3.87 ppm (s, 2H); ^{19}F NMR: δ = −150.3 ppm (s); ^{11}B NMR: δ = −0.23 ppm (s); FAB-MS: m/z (%): 160 (100) $[N_{222.1O2}]^+$, 87 (100) $[BF_4]^-$; elemental analysis calcd (%) for $C_9H_{22}BF_4NO$ (247.09): C 43.8, H 9.0, N 5.7; found: C 43.9, H 9.4, N 5.7.

Procedure for quaternary ammonium salts with bis(trifluoromethanesulfonyl)imide ([QA][TFSI]): The same procedure was followed as used for the [QA][R_FBF_3] salts, as described above, except commercial H[TFSI] was used instead of aqueous H[R_FBF_3].

***N*,*N*-Diethyl-*N*-methyl-*N*-(*n*-propyl)ammonium bis(trifluoromethanesulfonyl)imide (N_{1223}[TFSI])**: Yield: 85%, colorless liquid; ^{1}H NMR: δ = 1.02 (t, J = 7.4 Hz, 3H), 1.43 (t, J = 7.2 Hz, 2×3H), 1.90 (m, 2H), 3.18 (s, 3H), 3.38 (m, 2H), 3.55 ppm (q, J = 7.3 Hz, 2×2H); ^{19}F NMR: δ = −78.9 ppm (s); elemental analysis calcd (%) for $C_{10}H_{20}F_6N_2O_4S_2$ (410.4): C 29.3, H 4.9, N 6.8; found: C 29.1, H 4.9, N 6.9.

***N*-(*n*-Butyl)-*N*,*N*-diethyl-*N*-methylammonium bis(trifluoromethanesulfonyl)imide (N_{1224}[TFSI])**: Yield: 87%, colorless liquid; ^{1}H NMR: δ = 0.99 (t, J = 7.4 Hz, 3H), 1.42 (t, J = 7.2 Hz, 2×3H), 1.46 (t, J = 7.4 Hz, 2H), 1.84 (m, 2H), 3.18 (s, 3H), 3.43 (m, 2H), 3.56 ppm (q, J = 7.3 Hz, 2×2H); ^{19}F NMR: δ = −78.9 ppm (s); elemental analysis calcd (%) for $C_{11}H_{22}F_6N_2O_4S_2$ (424.42): C 31.1, H 5.2, N 6.6; found: C 31.1, H 5.3, N 6.6.

***N*,*N*,*N*-Trimethyl-*N*-(2-methoxyethyl)ammonium bis(trifluoromethanesulfonyl)imide ($N_{111\text{-}1O2}$[TFSI])**: Yield: 87%, white solid; ^{1}H NMR: δ = 3.39 (m, 4×3H), 3.80 (s, 2H), 3.96 ppm (s, 2H); ^{19}F NMR: δ = −78.9 ppm (s); elemental analysis calcd (%) for $C_8H_{16}F_6N_2O_5S_2$ (398.34): C 24.1, H 4.1, N 7.0; found: C 24.1, H 4.1, N 7.0.

***N*-Ethyl-*N*,*N*-dimethyl-*N*-(2-methoxyethyl)ammonium bis(trifluoromethanesulfonyl)imide ($N_{112\text{-}1O2}$[TFSI])**: Yield: 85%, colorless liquid; ^{1}H NMR: δ = 1.47 (t, J = 7.2 Hz, 3H), 3.31 (s, 2×3H), 3.39 (s, 3H), 3.67 (q, J = 7.2 Hz, 2H), 3.74 (t, J = 4.8 Hz, 2H), 3.94 ppm (s, 2H); ^{19}F NMR: δ = −78.9 ppm (s); elemental analysis calcd (%) for $C_9H_{18}F_6N_2O_5S_2$ (412.37): C 26.2, H 4.4, N 6.8; found: C 26.1, H 4.4, N 6.8.

***N*,*N*-Diethyl-*N*-methyl-*N*-(2-methoxyethyl)ammonium bis(trifluoromethanesulfonyl)imide ($N_{122\text{-}1O2}$[TFSI])**: Yield: 86%, colorless liquid; ^{1}H NMR: δ = 1.44 (t, J = 7.2 Hz, 2×3H), 3.24 (s, 3H), 3.39 (s, 3H), 3.62 (q, J = 7.3 Hz, 2×2H), 3.71 (t, J = 4.8 Hz, 2H), 3.92 ppm (s, 2H); ^{19}F NMR: δ = −78.9 ppm (s); elemental analysis calcd (%) for $C_{10}H_{20}F_6N_2O_5S_2$ (426.4): C 28.2, H 4.7, N 6.6; found: C 27.9, H 4.8, N 6.6.

***N*,*N*,*N*-Triethyl-*N*-(2-methoxyethyl)ammonium bis(trifluoromethanesulfonyl)imide ($N_{222\text{-}1O2}$[TFSI])**: Yield: 88%, colorless liquid; ^{1}H NMR: δ = 1.40 (t, J = 7.2 Hz, 3×3H), 3.38 (s, 3H), 3.57 (q, J = 7.2 Hz, 3×2H), 3.67 (t, J = 4.8 Hz, 2H), 3.89 ppm (s, 2H); ^{19}F NMR: δ = −78.9 ppm (s); elemental analysis calcd (%) for $C_{11}H_{22}F_6N_2O_5S_2$ (440.42): C 30.0, H 5.0, N 6.4; found: C 29.8, H 4.7, N 6.1.

Acknowledgement

This work was supported by R&D project for Li batteries by METI and NEDO of Japan. We are grateful to Ms Kazuko Igarashi and Ms Etsuko Hazama for their assistance in this work.

[1] a) D. Holbrey, K. R. Seddon, *Clean Prod. Process* **1999**, *1*, 223–236; b) T. Welton, *Chem. Rev.* **1999**, *99*, 2071–2084; c) P. Wasserscheid, W. Keim, *Angew. Chem.* **2000**, *112*, 3926–3945; *Angew. Chem. Int. Ed.* **2000**, *39*, 3772–3789; d) J. Dupont, R. F. de Souza, P. A. Z. Suarez, *Chem. Rev.* **2002**, *102*, 3667–3692.

[2] a) R. A. Sheldon, R. M. Lau, M. J. Sorgedrager, F. van-Rantwijk, K. R. Seddon, *Green Chem.* **2002**, *4*, 147–151; b) U. Kragel, M. Eckstein, N. Kaftzik, *Curr. Opin. Biotechnol.* **2002**, *13*, 565–571; c) S. Park, R. J. Kazlauskas, *Curr. Opin. Biotechnol.* **2003**, *14*, 432–437.

[3] a) C. C. Tzschucke, C. Markert, W. Bannwarth, S. Roller, A. Hebel, R. Haag, *Angew. Chem.* **2002**, *114*, 4136–4173; *Angew. Chem. Int. Ed.* **2002**, *41*, 3964–4000; b) C. F. Poole, *J. Chromatogr. A* **2004**, *1037*, 49–82.

[4] a) N. Nakagawa, S. Izuchi, K. Kuwana, T. Nukuda, Y. Aihara, *J. Electrochem. Soc.* **2003**, *150*, A695-A700; b) B. Garcia, S. Lavallee, G. Perron, C. Michot, M. Armand, *Electrochim. Acta* **2004**, *49*, 4583–4588.

[5] A. Weber, G. E. Blomgrem in *Advances in Lithium-Ion Batteries* (Eds.: W. A. Van Schalkwijk, B. Scrosati), Kluwer Academic/Plenum Publishers, New York, **2002**, pp. 185–232.

[6] a) P. Wang, S. M. Zakeeruddin, P. Comte, I. Exnar, M. Gratzel, *J. Am. Chem. Soc.* **2003**, *125*, 1166–1167; b) H. Matsumoto, T. Matsuda, T. Tsuda, R. Hagiwara, Y. Ito, Y. Miyazaki, *Chem. Lett.* **2001**, 26–27.

[7] W. Lu, A. G. Fadeev, B. Qi, E. Smela, B. R. Mattes, J. Ding, G. M. Spinks, J. Mazurkiewicz, D. Zhou, G. G. Wallace, D. R. MacFarlane, S. A. Forsyth, M. Forsyth, *Science* **2002**, *297*, 983–987.

[8] R. Hagiwara, Y. Ito, *J. Fluorine Chem.* **2000**, *105*, 221–227.

[9] H. Matsumoto, M. Yanagida, K. Tanimoto, M. Nomura, Y. Kitagawa, Y. Miyazaki, *Chem. Lett.* **2000**, 922–923; b) H. Matsumoto, H. Yanagida, K. Tanimoto, T. Kojima, Y. Tamiya, Y. Miyazaki in *Proc. Electrochem. Soc. (Molten Salts XII)*, *Vol. 99–41* (Eds.: P. C. Trulove, H. C. De Long, G. R. Stafford, S. Deki), **2000**, pp. 186–192; c) H. Matsumoto, H. Kageyama, Y. Miyazaki in *Proc. Electrochem. Soc. (Molten Salts XIII)*, *Vol. 2002–19* (Eds.: P. C. Trulove, H. C. De Long, R. A. Mantz, G. R. Stafford, M. Matsunaga), **2002**, pp. 1057–1065.

[10] H. Sakaebe, H. Matsumoto, *Electrochem. Commun.* **2003**, *5*, 594–598.

[11] J. H. Shin, W. A. Henderson, S. Passerini, *Electrochem. Commun.* **2003**, *5*, 1016–1020.

[12] P. C. Howlett, D. R. MacFarlane, A. F. Hollenkamp, *Electrochem. Solid-State Lett.* **2004**, *7*, A97-A101.

[13] T. Sato, G. Masuda, K. Takagi, *Electrochim. Acta* **2004**, *49*, 3603–3611.

[14] A. I. Bhatt, I. May, V. A. Volkovich, M. E. Hetherington, B. Lewin, R. C. Thied, N. Ertokc, *J. Chem. Soc. Dalton Trans.* **2002**, 4532–4534.

[15] a) J. E. Gordon, *J. Am. Chem. Soc.* **1965**, *87*, 4347–4358; b) J. E. Gordon, G. N. Subba Rao, *J. Am. Chem. Soc.* **1978**, *100*, 7445–7454; c) W. T. Ford, R. J. Hauri, D. J. Hart, *J. Org. Chem.* **1973**, *38*, 3916–3918.

[16] a) J. Sun, M. Forsyth, D. R. MacFarlane, *Ionics* 1997, *3*, 356–362; b) J. Sun, M. Forsyth, D. R. MacFarlane, *J. Phys. Chem. B* **1998**, *102*, 8858–8864; c) D. R. McFarlane, J. Sun, J. Golding, P. Meakin, M. Forsyth, *Electrochim. Acta* **2000**, *45*, 1271–1278.

[17] H. Matsumoto, H. Kageyama, Y. Miyazaki, *Chem. Lett.* **2001**, 182–183.

[18] J. E. Gordon in *Techniques and Methods of Organic and Organometallic Chemistry*, *Vol. 1* (Ed.: R. E. Denny), Marcel Dekker, New York, **1969**, pp. 51–188.

[19] a) E. I. Cooper, C. A. Angell, *Solid State Ionics* **1983**, *9/10*, 617–622; b) E. I. Cooper, C. A. Angell, *Solid State Ionics* **1986**, *18/19*, 570–576.

[20] M. Ue, K. Ida, S. Mori, *J. Electrochem. Soc.* **1994**, *141*, 2989–2996.

[21] M. Ue, M. Takeda, M. Takehara, S. Mori, *J. Electrochem. Soc.* **1997**, *144*, 2684–2688.

[22] K. Xu, M. S. Ding, T. R. Jow, *J. Electrochem. Soc.* **2001**, *148*, A267-A274.

[23] S. Forsyth, J. Golding, D. R. MacFarlane, M. Forsyth, *Electrochim. Acta* **2001**, *46*, 1753–1757.

[24] J. Golding, N. Hamid, D. R. MacFarlane, M. Forsyth, C. Forsyth, C. Collins, J. Huang, *Chem. Mater.* **2001**, *13*, 558–564.

[25] W. Xu, E. I. Cooper, C. A. Angell, *J. Phys. Chem. B* **2003**, *107*, 6170–6178.

[26] W. Xu, L. M. Wang, R. A. Nieman, C. A. Angell, *J. Phys. Chem. B* **2003**, *107*, 11749–11756.

[27] H. Matsumoto, H. Kageyama, Y. Miyazaki, *Chem. Commun.* **2002**, 1726–1727.

[28] D. R. MacFarlane, J. Golding, S. Forsyth, M. Forsyth, G. B. Deacon, *Chem. Commun.* **2001**, 1430–1431.

[29] D. R. MacFarlane, P. Meakin, J. Sun, N. Amini, M. Forsyth, *J. Phys. Chem. B.* **1999**, *103*, 4164–4170.

[30] P. Lozano, T. de Diego, S. Gmouh, M. Vaultier, J. L. Iborra, *Biotechnol. Prog.* **2004**, *20*, 661–669.

[31] a) O. D. Gupta, P. D. Armstrong, J. M. Shreeve, *Tetrahedron Lett.* **2003**, *44*, 9367–9370; b) J. Kim, R. P. Singh, J. M. Shreeve, *Inorg. Chem.* **2004**, *43*, 2960–2966.

[32] K. Kim, S. Choi, D. Demberelnyamba, H. Lee, J. Oh, B. Lee, S. Mun, *Chem. Commun.* **2004**, 828–829.
[33] a) A. P. Abbott, G. Capper, D. L. Davies, R. Rasheed, *Inorg. Chem.* **2004**, *43*, 3447–3452; b) P. Abbott, G. Capper, D. L. Davies, H. L. Munro, R. K. Rasheed, V. Tambyrajah, *Chem. Commun.* **2001**, 2010–2011.
[34] M. Armand, W. Gorecki, R. Andreani, in *Second International Symposium on Polymer Electrolytes* (Ed.: B. Scrosati), Elsevier, London, **1990**, p. 91–97.
[35] a) P. Johansson, S. P. Gejji, J. Tegenfeldt, J. Lindgren, *Electrochim. Acta* **1998**, *43*, 1375–1379; b) P. Johansson, P. Jacobsson, *J. Phys. Chem. A* **2001**, *105*, 8504–8509.
[36] a) V. P. W. Bohm, W. A. Herrmann, *Chem. Eur. J.* **2000**, *6*, 1017–1025; b) G. Zou, Z. Wang, J. Zhu, J. Tang, M. Y. He, *J. Mol. Catal. A: Chem.* **2003**, *206*, 193–198.
[37] H. J. Frohn, V. V. Bardin, *Z. Anorg. Allg. Chem.* **2001**, *627*, 15–16.
[38] Z. B. Zhou, M. Takeda, M. Ue, *J. Fluorine Chem.* **2003**, *123*, 127–131.
[39] A. A. Kolomeitsev, A. A. Kadyrov, J. Szczepkowska-Sztolcman, M. Milewska, H. Koroniak, G. Bissky, J. A. Barten, G. V. Roschenthaler, *Tetrahedron Lett.* **2003**, *44*, 8273–8277.
[40] G. A. Molander, B. P. Hoag, *Organometallics* **2003**, *22*, 3313–3315.
[41] a) V. V. Bardin, S. G. Idemskaya, H. J. Frohn, *Z. Anorg. Allg. Chem.* **2002**, *628*, 883–890; b) M. Takeda, M. Takehara, M. Ue (Mitsubishi Chem.), JP63934A, **2002**; c) M. Schmidt, A. Kuhner, K.-D. Franz, G.-V. Roschenthaler, G. Bissky, A. Kolomeitsev, A. Kadyrov (Merck GmbH), US0160261A1, **2002**.
[42] a) V. V. Bardin, H. J. Frohn, *Main Group Met. Chem.* **2002**, 25, 589–613; b) G. Pawelke, H. Burger, *Coord. Chem. Rev.* **2001**, 215, 243–266.
[43] Z. B. Zhou, M. Takeda, M. Ue, *J. Fluorine Chem.* **2004**, *125*, 471–476.
[44] Z. B. Zhou, H. Matsumoto, K. Tatsumi, *Chem. Lett.* **2004**, 680–681.
[45] Z. B. Zhou, H. Matsumoto, K. Tatsumi, *Chem. Eur. J.* **2004**, *10*, 6581–6591.
[46] Z. B. Zhou, H. Matsumoto, K. Tatsumi, *Chem. Lett.* **2004**, 886–887.
[47] K. R. Seddon, A. Stark, M. J. Torres, *Pure Appl. Chem.* **2000**, *72*, 2275–2287.
[48] J. Timmermans, *J. Phys. Chem. Solids* **1961**, *18*, 1–8.
[49] a) D. MacFarlane, J. Huang, M. Forsyth, *Nature* **1999**, *402*, 792–794; b) D. MacFarlane, M. Forsyth, *Adv. Mater.* **2001**, *13*, 957–966; c) D. MacFarlane, P. Meakin, N. Amini, M. Forsyth, *J. Phys. Condens. Matter* **2001**, *13*, 8257–8267.
[50] a) A. Abouimrane, Y. Abu-Lebdeh, P. J. Alarco, M. Armand, *J. Electrochem. Soc.* **2004**, *151*, A1028–A1028; b) Y. Abu-Lebdeh, P. J. Alarco, M. Armand, *Angew. Chem.* **2003**, *115*, 4637–4639; *Angew. Chem. Int. Ed.* **2003**, *42*, 4499–4501.
[51] a) J. C. Dearden, *Sci. Total Environ.* **1991**, *109/110*, 59–68; b) R. Abramowitz, S. H. Yalkowsky, *Pharm. Res.* **1990**, *7*, 942–947.
[52] W. Xu, C. A. Angell, *Electrochem. Solid-State Lett.* **2001**, *4*, E1-E4.
[53] D. Aurbach, H. Gottlieb, *Electrochim. Acta* **1989**, *34*, 141–156.
[54] U. Schroder, J. D. Wadhawan, R. G. Compton, F. Marken, P. A. Z. Suarez, C. S. Consorti, R. F. de Souza, J. Dupont, *New J. Chem.* **2000**, *24*, 1009–1015.

Received: August 10, 2004
Published online: December 6, 2004